Journal of Sound and Vibration (2000) **231**(2), 307–341
doi:10.1006/jsvi.1999.2720, available online at http://www.idealibrary.com on IDEAL®

PHASE-SPACE LINEARIZATION FOR NON-LINEAR OSCILLATORS: DETERMINISTIC AND STOCHASTIC SYSTEMS

D. ROY

Structural Engineering Division, Department of Civil Engineering, Indian Institute of Technology, Kharagpur 721 302, *India*

(*Received* 1 *April* 1999, *and in final form* 10 *September* 1999)

A new and efficient semi-analytical phase-space linearization (PSL) scheme for a class of non-linear oscillators is developed in this paper. The method is based on replacement of the non-linear vector field by a set of linear ones, each valid over a short segment of the evolving trajectory or over sufficiently small interval of time. Based on this concept, a few explicit and implicit integration schemes are first proposed and applied to a class of low-dimensional non-linear dynamical systems to accurately determine their response trajectories. This approach of local linearization is further extended to non-linear oscillators excited by formal derivatives of one or a combination of Gauss–Markov processes. Since the present methodology reduces the non-linear operator by a set of linear operators, it is also demonstrated that the principles of linear random vibration may be suitable exploited to arrive at a faster and semi-analytical Monte-Carlo scheme for computing the response statistics, both in stationary and non-stationary regimes. Limited examples are presented and compared with exact solutions whenever available, to illustrate the efficiency and versatility of the proposed schemes.

1. INTRODUCTION

Recently, Iyengar and Roy [1, 2] proposed a phase-space linearization (PSL) method to decompose a given non-linear system into a set of linear ones, each representing the original system locally over a short segment of the evolving trajectory in the associated phase space. The PSL method was found to be versatile enough to accurately predict a wide variety of response patterns, such as one- or multi-periodic, almost periodic, quasi-periodic and chaotic. A procedure based on locally defined least-squares error minimization was suggested to derive the set of linearized equations. It was further pointed out that the procedure to derive such locally linearized ordinary differential equations (ODEs) was not unique and thus merited further attention. In case the system along with the excitations are deterministic, the local error minimization scheme led to a set of non-linear algebraic equations for the unknown coefficients, which in turn are required to construct the linearized ODEs. It may however be observed that such a scheme becomes unwieldy when the system is driven by stochastic or a combination of

0022-460X/00/120307 + 35 $35.00/0

deterministic and stochastic excitations. It is therefore a necessity to explore other forms of linearization principles within the framework of PSL, so that the response scenario of non-linear oscillators in a stochastic regime can be conveniently explored [3].

In very much the same way a deterministic non-linear oscillator exhibits chaos and addition of random noise may induce the system to exhibit stochastic chaos as well. As has been shown by Simiu and Frey [4], an oscillator having a homoclinic orbit in the unperturbed phase space may undergo a series of homoclinic bifurcations finally leading to stochastic chaos under external stochastic perturbations. A contradictory scenario, in which addition of a small quasiperiodic noise may decrease the zones of existence of each of the period-doubled orbits, has also been reported by Kapitaniak [5, 6]. Non-linear oscillators are generically non-integrable and thus exact sample solutions for the stochastic flow are ruled out. For systems driven by Gaussian white noise, solutions of the associated Fokker Planck equation, even under the assumption of stationarity, are also rarely possible [7]. This emphasizes in no uncertain terms the usefulness of numerical or semi-analytical algorithms for the study of response behaviour of a general non-linear dynamical system of engineering importance. Stochastic counterparts of many of the deterministic numerical integration procedures, such as Euler, Runge–Kutta of different orders, etc., are available [8, 9]. More recently, Askar *et al.* [10] proposed a faster simulation method based on a piecewise linearization of non-linear drift coefficients. The method, however, does not reflect on the accuracy of pathwise solutions of response trajectories.

The present study is aimed at developing, within the broad framework of PSL, a robust semi-analytical algorithm based on pathwise and segmented linearizations of associated vector fields to integrate non-linear ODEs under deterministic and stochastic excitations. Such a representation not only helps in efficient integration, but also in a better physical understanding of the underlying dynamical behaviour using the well-established theories in linear dynamics. Towards this, a few implicit and explicit schemes are first proposed for deterministic systems along with some numerical examples and comparisons with computer simulations. The explicit scheme is next extended for non-linear oscillators driven by a combination of deterministic and stochastic excitations. The stochastic excitations considered in this study are white-noise processes, described by formal time derivatives of Gaussian Wiener processes. The essence of the explicit linearization procedure is to use a short-time-averaged Ito–Taylor or Wagner–Platen expansion for replacing the non-linear terms in the vector field by linear ones. Based on this, a direct simulation procedure is formalized for computing response statistics of non-linear dynamical systems. Further, it is shown that one can suitably exploit the set of linearized vector fields, each valid over short trajectory segments, to solve for associated Fokker–Planck equations in closed form. The corresponding transition probability density (TDP) is Gaussian given the sharp values of the state variables at the immediately preceding time instant. Limited numerical illustrations of the method are provided. The advantage of the present schemes over the usual path integral formalism, based on an expansion of the Fokker–Planck equation over a short time interval [11, 12], is also briefly touched upon.

2. THE CONCEPT OF LINEARIZATION

The concept of local linearizations of vector fields around fixed points, or more generally non-wandering sets, is well studied in the literature on non-linear dynamical systems [13, 14]. In particular, it is known from Hartman's theorem that if p is a hyperbolic fixed point of the non-linear oscillator, then there exists a C^0 homeomorphism locally taking the actual orbits to the orbit of the linearized variational equation, defined by

$$\dot{Y} = D_X(p)\, Y, \tag{1}$$

where X is the original co-ordinate vector. However, there is no way to explicitly construct this homeomorphism and, moreover, away from the fixed point, p, Hartman's theorem is no longer valid. The extension of Hartman's theorem for the stochastic case is also available. Even though helpful in establishing a correspondence between linear and non-linear flows, such theorems are not sufficient to establish a numerical procedure to simulate a non-linear flow using some suitably linearized flow, even near fixed invariant sets.

3. A NEW PATHWISE LINEARIZATION SCHEME

To start with, consider the following non-linear ODE:

$$\{\dot{x}\} = \{f(\{x\}, t), \qquad \{x\} \in U \subset R^n, \quad t \in R \tag{2}$$

subjected to initial conditions

$$\{x(t_0)\} = \{x_0\}, \tag{3}$$

If the vector field $\{f\}$ is C^r, $r \geqslant 1$ and $(\{x_0\}, t_0\} \in U \subset R^n \times R^1$, then according to the existence and uniqueness theorem [14], there is a unique C^r local solution $\{x(\{x_0\}, t_0, t)\}$ for $|t - t_0|$ sufficiently small. Moreover, the solution $\{x(\{x_0\}, t_0, t)\}$ can be extended backward and forward in time provided that it is bounded. Now, for convenience of discussion, the following class of ODEs is considered:

$$\{\ddot{x}\} + [c]\{\dot{x}\} + [k]\{x\} + \{\xi(\{x\}, \{\dot{x}\}\} = \{F\}, \quad x \in R^n \tag{4}$$

with the initial conditions

$$\{x(t_0)\} = \{x_0\}, \qquad \{\dot{x}(t_0)\} = \{\dot{x}_0\}. \tag{5}$$

Here $\{F\}$ is a vector-valued sinusoidal function with typical elements $F_i = A_i \sin(\lambda_i t)$. However, it may be mentioned here that the discussion to follow covers an even wider class of non-linear oscillators. Let the vector function $\{\xi\}$ be C^r, $r \geqslant 1$, over the full range of state variables. Then the solution vector $\{\{x\}, \{\dot{x}\}\}^{\mathrm{T}}$ will also be C^r in t. At this stage, it is convenient to order the time axis as

$t_0 < t_1 < t_2 < \cdots < t_i < t_{i+1} < \cdots$. Let the corresponding points on a solution trajectory be denoted as $\{X_i\} = \{\{x\}, \{\dot{x}\}\}^{\mathrm{T}}$, $i = 0, 1, 2...$ A knowledge of the closed–open solution segment $S_i = [\{X_i\}, \{X_{i+1}\}) \in R^{2n}$ allows one to construct the complete solution trajectory starting at $\{X_0\}$ by taking the union $\bigcup_i S_i$. The objective is to obtain a representation for the solution segment S_i in terms of linear ODEs, derivable from the originally non-linear ODE.

Now, over the semi-closed time interval $T_i = [t_i, t_{i+1}]$, the C^r solution trajectory allows a Fourier series representation following the Stone–Weierstrass theorem [15] and thus it may be argued that over the same time interval it is possible to replace the non-linear ODE via an equivalent linear ODE, since the same Fourier representation is obtainable from a linear system. In other words, the space of solutions of the locally linearized system is dense in the space of all C^r functions over S_i. However, deriving such linear systems over each time interval is not unique. Presently, in what follows, two different schemes, explicit and implicit, are proposed.

3.1. AN EXPLICIT SCHEME

First, it is assumed that the non-linear vector field of jth equation can be decomposed as

$$\xi_j(\{x\}, \{\dot{x}\}) = \sum_{k=1}^{n} \beta_{jk}(\{x\}, \{\dot{x}\}) x_k + \sum_{k=1}^{n} \kappa_{jk}(\{x\}, \{\dot{x}\}) \dot{x}_k, \quad k = 1, 2, \ldots, n. \tag{6}$$

It is also assumed that interval S_i is small enough to expand the functions β_{jk} and κ_{jk} in deterministic Taylor series and that $\lim_{\{X\} \to \{\bar{X}\}} \beta_{jk}(\bar{X})$, and $\lim_{\{X\} \to \{\bar{X}\}} \kappa_{jk}(\bar{X})$ exist and are finite for all points of singularity $\{X\} = \{\bar{X}\}$ of the functions with j, $k = 1, 2, 3, \ldots, n$. Now deterministic Taylor expansions of these functions about the point $\{X(t_i)\} = \{X_i\}$, $t \geqslant t_i$ may be expressed as

$$\beta_{jk}(\{X\}, t) = \beta_{jk}(\{X_i\}, t_i) + \sum_{l=1}^{2n} \frac{\partial \beta_{jk}(\{X_i\}, t_i)}{\partial X_l} (t - t_i)$$

$$+ (1/2!) \sum_{l,m=1}^{2n} \frac{\partial^2 \beta_{jk}(\{X_i\}, t_i)}{\partial X_l \partial X_m} (t - t_i)^2 + \cdots + \mathfrak{R} \tag{7}$$

and similarly for κ_{jk}. Here the term $\mathfrak{R}$ on the RHS of the above equation denotes the remainder set and $t \in T_i$. In the above equation, only three terms have been included in the hierarchical set. However, for better precision within a given time interval, more terms in the Taylor expansion may be included. At this stage, it is convenient to introduce a non-negative measure of the set T_i as

$$h_i = t_{i+1} - t_i \in R^+. \tag{8}$$

It may now be readily observed that for any $i \in [0, \infty)$, h_i may be chosen to be sufficiently small such that over T_i the variations of β_{jk} and κ_{jk} are either small or

negligible. Thus, it is possible to average out the explicit time dependence of these functions over T_i to arrive at the following constant approximations of β_{jk} and κ_{jk}, respectively,

$$\bar{\beta}_{jk} = (1/h_i) \int_{t_i}^{t_i + h_i} \beta_{jk}(\{X_i\}, s)\, \mathrm{d}s, \qquad \bar{\kappa}_{jk} = (1/h_i) \int_{t_i}^{t_i + h_i} \kappa_{jk}(\{X_i\}, s)\, \mathrm{d}s. \tag{9}$$

With this approximation, it is possible to replace the originally non-linear ODE (equation (4)) by the following time-invariant ODE with constant coefficient deemed to be valid uniformly over the time segment T_i:

$$\{\ddot{y}\} + [c]\{\dot{y}\} + [\bar{\kappa}(\{X_i\})]\{\dot{y}\} + [k]\{y\} + [\bar{\beta}(\{X_i\})]\{y\} = \{F\}, \tag{10}$$

where $[\bar{\beta}(\{X_i\}]$, and $[\bar{\kappa}(\{X_i\})]$ are, in general, $n \times n$ non-symmetric (possibly sparse) matrices with typical elements $\bar{\beta}_{jk}$ and $\bar{\kappa}_{jk}$, respectively, and the initial conditions to the above equations are $\{Y(t_i)\} = \{Y_i\} = \{X_i\}$. Thus, the above system of ODEs are conditionally linear given the initial values of the state variables at the start of the interval. This would enable one to locally integrate these linear ODEs to have a local approximation to the solution of the non-linear ODE over T_i. The complete solution is then obtained by joining the local solutions together.

3.2. AN IMPLICIT SCHEME

In what follows, an approximate replacement technique for the vector-valued non-linear function $\{\xi_j(\{X\}) | j = 1, 2, 3, \ldots, n\}$ based on the minimization of errors is indicated [1, 2]. Here in the semi-closed interval T_i, equation (4) is replaced by the following system of conditionally linear ODEs:

$$\{\ddot{x}\} + [c]\{\dot{x}\} + [k]\{x\} + [K(\{X_i\})]\{x\} + [C(\{X_i\})]\{\dot{x}\} = \{F\}, \tag{11}$$

where the matrices $[K]$ and $[C]$ are diagonal $n \times n$ diagonal matrices with the jth diagonal entry given by K_j and C_j respectively. Now, square of each element of the error vector $\{e_i\} = \{e_{1,i}\, e_{2,i} \cdots e_{n,i}\}^{\mathrm{T}}$ over time interval T_i:

$$e_{j,i}^2 = \int_{\{x_i\}}^{\{x_i\} + \{\Delta_i\}} \int_{\{\dot{x}_i\}}^{\{\dot{x}_i\} + \{\gamma_i\}} (\xi_j(\{X\}) - K_j x_j - C_j \dot{x}_j)^2\, \mathrm{d}x_j\, \mathrm{d}\dot{x}_j \tag{12}$$

may be minimized with respect to the unknown parameters K_j and C_j in the following way for each i:

$$\partial e_{j,i}^2 / \partial K_j = \partial e_{j,i}^2 / \partial C_j = 0. \tag{13}$$

In equation (12), the jth elements of vector increments $\{\Delta_i\}$ and $\{\gamma_i\}$ are given by

$$(\Delta_j)_i = (x_j)_{i+1} - (x_j)_i, \qquad (\gamma_j)_i = (\dot{x}_j)_{i+1} - (\dot{x}_j)_i. \tag{14}$$

Equations (13) and (14) together lead to $2n$ non-linear algebraic equations in $2n$ unknown quantities $\Delta_j, \gamma_j, j = 1, 2, \ldots, n$ for each i. In the special cases where the vector function elements $\xi_j, j = 1, 2, 3, \ldots, n$, are of one of the following forms:

$$\xi_j = \xi_j(\{x\}), \qquad \xi_j = \xi_j(\{\dot{x}\}), \quad \xi_j = \mu_1(\{\dot{x}\})x_j, \qquad \xi_j = \mu_2(\{x\})\dot{x}_j \tag{15}$$

only a set of n non-linear algebraic equations for $\Delta_j, \gamma_j, j = 1, 2, \ldots, n$, need to be solved for each j.

3.3. ILLUSTRATIVE EXAMPLES

To illustrate the implementation of the above linearization schemes, a commonly used non-linear single-degree-of-freedom (s.d.o.f.) oscillator, namely the hardening Duffing oscillator is taken up. It may be mentioned that this oscillator is non-hyperbolic in the phase space when it is not perturbed by forcing and damping. However, with a suitable choice of parameters and both damping and external forcing terms included, the Duffing oscillator even shows chaos. After suitable normalizations, the oscillator is given by the following non-linear second order ODE:

$$\ddot{x} + 2\pi\varepsilon_1\dot{x} + 4\pi^2\varepsilon_2(1 + x^2)x = 4\pi^2\varepsilon_3\cos(2\pi t). \tag{16}$$

Now, according to the notations followed here, it is observed that $n = 2$, $[c]$ and $[k]$ are scalar quantities with $c = 2\pi\varepsilon_1$, $k = 4\pi^2\varepsilon_2$, $\xi(x) = 4\pi^2\varepsilon_2 x^2$. Using the concept of pathwise linearization, the conditionally linear equivalent ODE, valid over T_i takes the form

$$\ddot{y} + 2\pi\varepsilon_1\dot{y} + 4\pi^2\varepsilon_2\beta y = 4\pi^2\varepsilon_3\cos(2\pi t). \tag{17}$$

The explicit scheme: In this scheme, β is obtained by expanding x^2 locally around the point $\{x_i, \dot{x}_i, t\}$ in a Taylor series followed by time averaging over the interval $h_i = t_{i+1} - t_i$. This leads to the following expression for β:

$$\beta(x_i, \dot{x}_i, h_i) = 1 + x_i^2 + x_i\dot{x}_i h_i + (\tfrac{1}{3})(\dot{x}_i^2 + x_i\ddot{x}_i)h_i^2 + \Re(O(h_i^3)), \tag{18}$$

where $\ddot{x}_i$ is given by

$$\ddot{x}_i = -2\pi\varepsilon_1\dot{x}_i - 4\pi^2\varepsilon_2\beta x_i + 4\pi^2\xi_3\cos(2\pi t_i). \tag{19}$$

At this point, it may be noted that the above procedure does not ensure the positivity of β. To ensure this, one may expand x about x_i, square the resulting quantity and finally average it over T_i to arrive at a strictly non-negative expression. Thus, for example, taking a three-term hierarchical expansion for

x about x_i, one obtains the following non-hierarchical expression for β:

$$\beta(x_i, \dot{x}_i, h_i) \cong 1 + x_i^2 + x_i\dot{x}_i h_i + (\tfrac{1}{3})(\dot{x}_i^2 + x_i\ddot{x}_i)h_i^2 + x_i\ddot{x}_i h_i^3/4 + \dot{x}_i^4/20. \quad (20)$$

In fact, ensuring positivity of some crucial terms may be of use in an error analysis. The pair of eigenvalues associated with the complimentary function of equation (17) are

$$^i\lambda_{1,2} = -\pi\varepsilon_1 \pm \pi\sqrt{(\varepsilon_1^2 - 4\varepsilon_2\beta)}. \quad (21)$$

Now, the particular solution of equation (17) is

$$p_i(t) = \frac{\varepsilon_3(\varepsilon_2\beta - 1)\cos(2\pi t) + \varepsilon_1\varepsilon_3 \sin(2\pi t)}{(\varepsilon_2\beta - 1)^2 + \varepsilon_1^2}. \quad (22)$$

The complete solution of equation (17) may be written as

$$y(t) = F_{1i}(x_i, \dot{x}_i, h_i) \qquad \dot{y}(t) = \mathrm{d}F_{1i}/\mathrm{d}t = F_{2i}(x_i, \dot{x}_i, h_i), \quad (23)$$

where

$$F_{1i} = A_{1i}\exp\{^i\lambda_1(t - t_i)\} + A_{2i}\exp\{^i\lambda_2\exp(t - t_i)\} + p_i(t),$$

$$F_{2i} = {}^i\lambda_1 A_{1i}\exp\{^i\lambda_1(t - t_i)\} + {}^i\lambda_2 A_{2i}\exp\{^i\lambda_2\exp(t - t_i)\} + \dot{p}_i(t), \quad (24)$$

if $^i\lambda_{1,2}$ are real, otherwise

$$F_{1i} = \exp\{-\pi\varepsilon_1(t - t_i)\}\{A_{1i}\cos(\pi\alpha_i t) + A_{2i}\sin(\pi\alpha_i t)\} + p_i(t),$$

$$F_{2i} = -\pi\varepsilon_1\exp\{-\pi\varepsilon_1(t - t_i)\}\{A_{1i}\cos(\pi\alpha_i t) + A_{2i}\sin(\pi\alpha_i t)\}$$

$$+ \pi\alpha_i\exp\{-\pi\varepsilon_1(t - t_i)\}\{A_{2i}\cos(\pi\alpha_i t) + A_{1i}\sin(\pi\alpha_i t)\} + \dot{p}_i(t),$$

$$\alpha_i = \sqrt{4\varepsilon_2\beta - \varepsilon_1^2}. \quad (25)$$

The constant A_{1i} and A_{2i} need to be determined from a knowledge of $\{x_i, \dot{x}_i\}$ followed by solving a pair of simultaneous equations.

The implicit scheme: Following an error minimization as explained earlier, i.e., $\partial^2 e/\partial\beta = 0$, the expression for β is found to be

$$\beta(x_i) = 1 + (x_i^4 + 2xx_i^3\Delta_i + 2x_i^3\Delta_i + x_i\Delta_i^3 + \Delta_i^4/5)/(x_i^2 + x_i\Delta_i + \Delta_i^2/3), \quad (26)$$

where $\Delta_i = x_{i+1} - x_i$. The approximate solution vector $\{y_{i+1}, \dot{y}_{i+1}\}$ at time $t = t_i$ may be constructed in precisely the same way as in the explicit case (now, as

a function of Δ_i). Finally, Δ_i may be solved from the following transcendental equation:

$$y_{i+1} \cong x_{i+1}(x_i, \dot{x}_i, h_i, \Delta_i) = x_i + \Delta_i. \tag{27}$$

Other implicit schemes may also be derived based on suitable choices for β as functions of x_i and x_{i+1}. One such choice may be

$$\beta = \sqrt{0{\cdot}5(x_i + x_{i+1})^2}. \tag{28}$$

Such an approach is however computationally more involved in that it requires solution of two non-linear algebraic equations for each i and hence is not further elaborated upon in the present work.

3.4. NUMERICAL RESULTS

It is now appropriate to present a few numerical results to substantiate the developments presented so far. In Figure 1, the phase plots of the unforced and undamped hardening Duffing oscillator as given by equation (16) are plotted using the explicit version of the short time linearization (STL) procedure and different number of terms, N, in the short-time-averaged Taylor expansion. In the same figure, these results are compared with the ones obtained using a sixth order Runge–Kutta scheme. It is observed that even using two terms in the expansion leads to highly favourable agreements with the results obtained via the

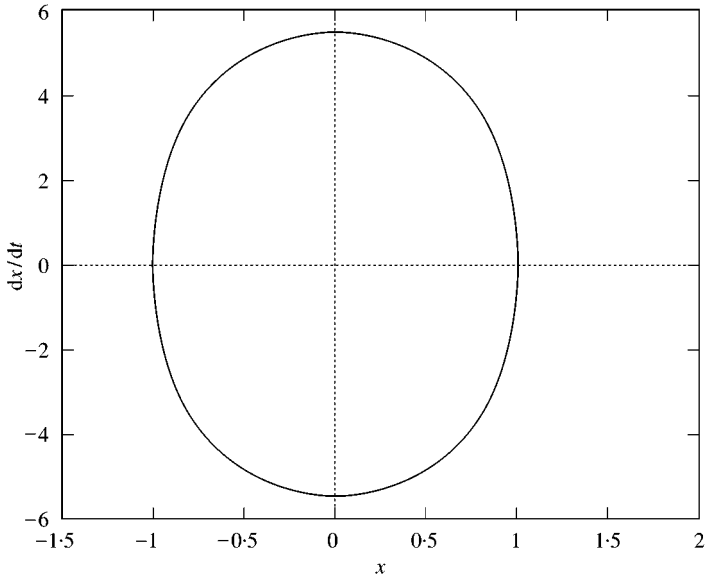

Figure 1. Phase plot of undamped and unforced Duffing's oscillator, $\varepsilon_2 = 0{\cdot}5$, $x_0 = 1{\cdot}0$, $\dot{x}_0 = 0{\cdot}1$, $h = 0{\cdot}002$: STL: $N = 2$ ——; STL: $N = 3$ – – – –; STL: $N = 4$ - - - - -; STL: $N = 5$ ·····; STL: $N = 6$ – · – · –; RKGS - - - .

Runge–Kutta scheme. In Figure 2, a one-periodic orbit, obtained via both the present and Runge–Kutta schemes, is shown. It is known that for certain parameter ranges, the hardening Duffing oscillator exhibits chaos [5] and phase plots of one such chaotic orbit are shown in Figure 3 for an increasing number of terms in the averaged Taylor expansion and with $h = 0{\cdot}01$ expect for Figure 3(a) where $h = 0{\cdot}002$. In the same figure, also shown is the chaotic orbit obtained via a sixth order Runge–Kutta scheme with $h = 0{\cdot}002$. It is again observed that the use of even two terms in the Taylor series is sufficient to capture the strange attractor. However, it may be mentioned that use of two terms requires a very short time step, $h = O(10^{-3})$ for prediction of chaotic orbits. The phase plot of a chaotic orbit using STL with $N = 2$ and $h = 0{\cdot}01$ is shown in Figure 4(a) and is found to be quite inaccurate. It may also be noted that even a sixth order Runge–Kutta scheme with $h = 0{\cdot}01$ also fails to obtain accurately the chaotic orbit, as shown in Figure 4(b). It is worth mentioning here that like the explicit scheme, implicit schemes also lead to similar results. These schemes have, however, been explored by Iyengar and Roy [1, 2] and are therefore not touched upon here.

It is readily observed that the coefficient $\beta(x_i, \dot{x}_i, \varepsilon_1, \varepsilon_2, \varepsilon_3, h_i, t_i)$ in the linearized equation (17) plays a crucial role in determining the accuracy of the new linearization procedure. Of particular interest would be the convergence of this conditionally constant coefficient β with the number of terms, N, in the short-time-averaging procedure. A few parametric studies for both periodic and chaotic parameter values are reported in Figure 5, where β is plotted against time step h_i. It may be seen that for $h_i \leqslant 0{\cdot}01$ even a two-term approximation

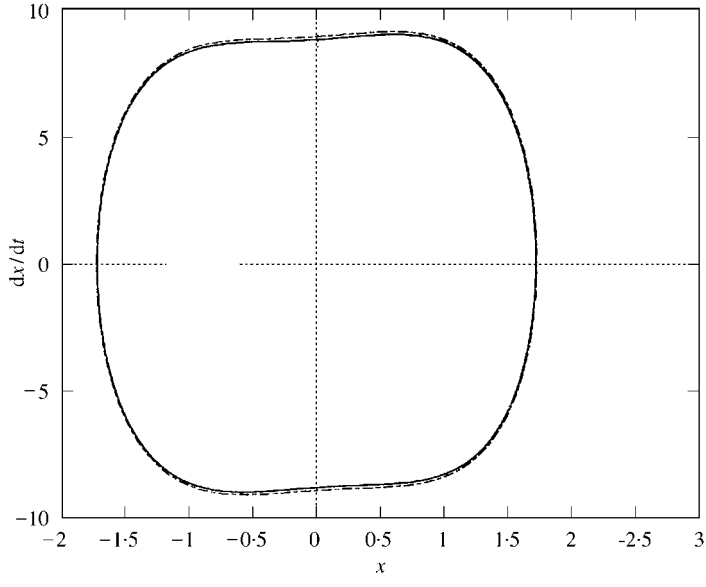

Figure 2. One-periodic limit cycle for Duffing's oscillator, $\varepsilon_2 = 0{\cdot}25$, $\varepsilon_2 = 0{\cdot}5$, $\varepsilon_3 = 1$, $h = 0{\cdot}002$: STL: $N = 2$ ——; STL: $N = 3$ – – – –; STL: $N = 4$ - - - - -; STL: $N = 5$ ·····; STL: $N = 6$ –·–·–; RKGS –·· .

predicts β accurately enough. However, for parameter values corresponding to a chaotic case, it is observed that higher values of h_i may result in considerable inaccuracy in the predicted response. An even more interesting result is reported in Figure 6 where the coefficient β has been plotted against the immediately preceding

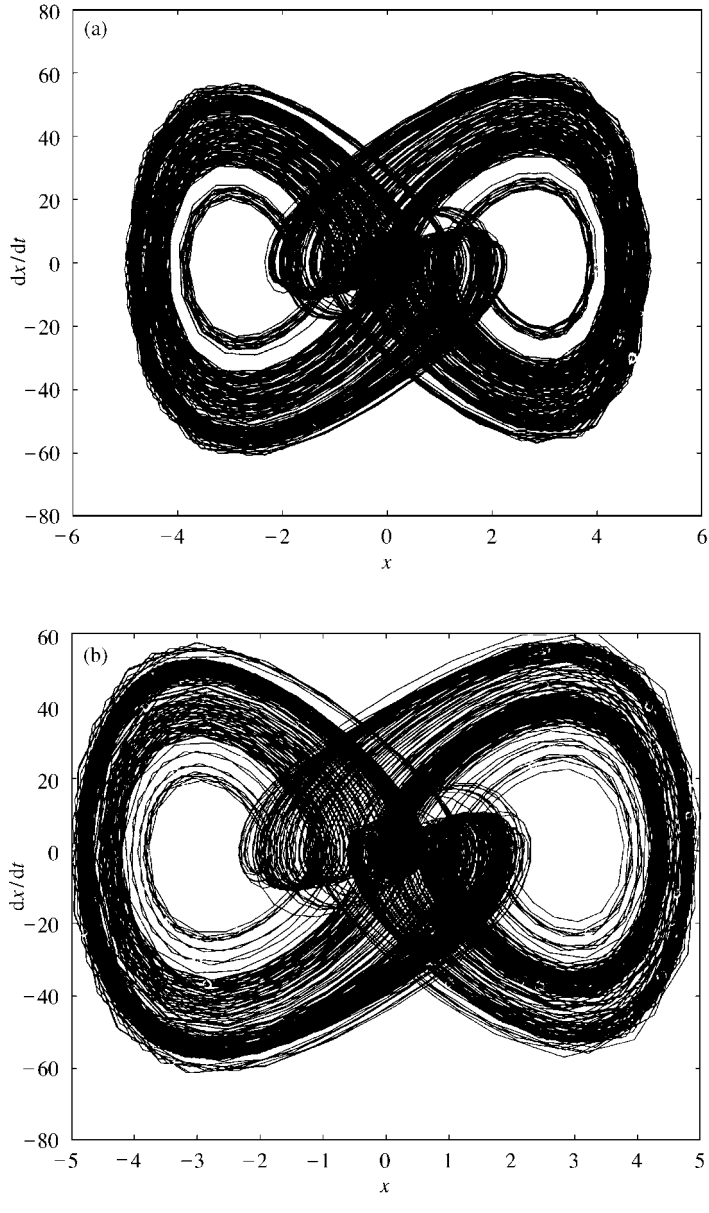

Figure 3. A typical chaotic orbit for Duffing's oscillator, $\varepsilon_1 = 0{\cdot}2$, $\varepsilon_2 = 0{\cdot}51$, $\varepsilon_3 = 15.3$. (a) Two terms in the averaged Taylor's expansion, $h = 0{\cdot}002$, (b) three terms in the averaged Taylors expansion, $h = 0{\cdot}01$, (c) four terms in the averaged Taylors expansion, $h = 0{\cdot}01$, (d) five terms in the averaged Taylors expansion, $h = 0{\cdot}01$, (e) six terms in the averaged Taylors expansion, $h = 0{\cdot}01$, (f) simulation by Runge–Kutta (sixth order) scheme, $h = 0{\cdot}002$.

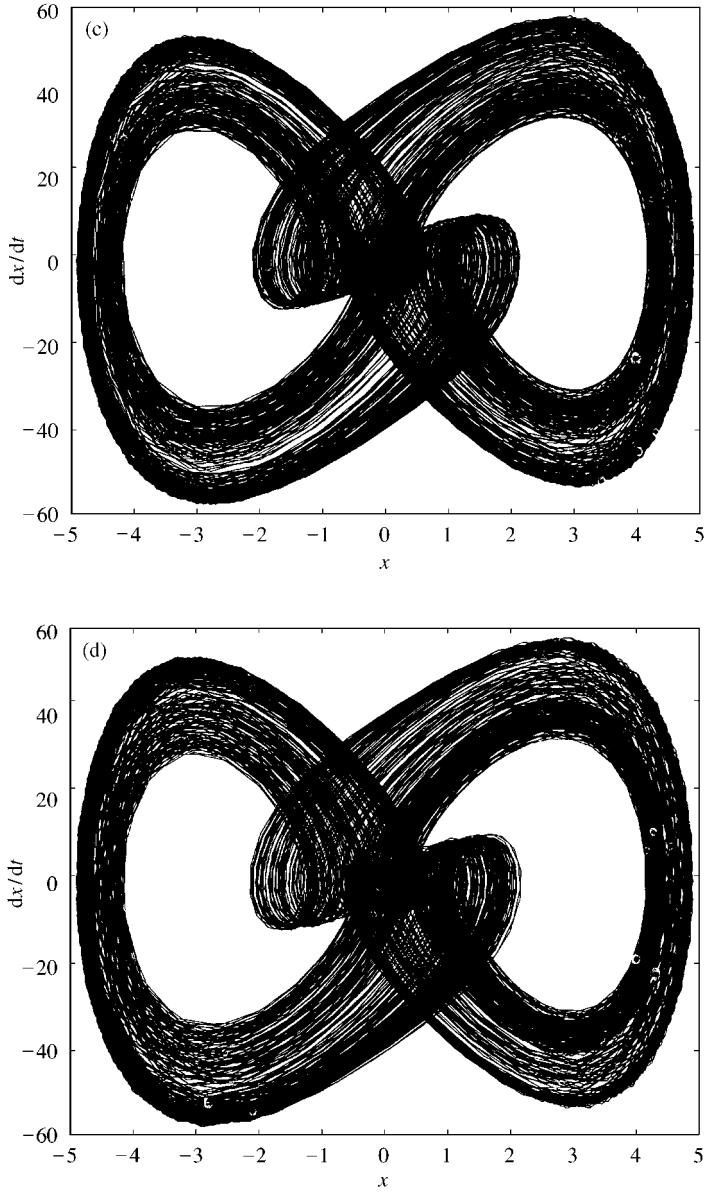

Figure 3. Continued.

time-instant t_i. It may be seen that for fixed values of all other parameters, the fluctuation of β is considerable in the chaotic regime and almost negligible in the periodic regime. This is more clearly seen in the 3-D surface plots β–x_i–t_i, as shown in Figures 7(a) and 7(b), and β–$\dot{x}_i$–t_i, and shown in Figures 7(c) and 7(d), for both periodic and chaotic regimes with six terms in the short-time-averaging procedure. This observation is in consonance with the known fact that the classical equivalent linearization procedure works well for the strictly periodic cases, where the

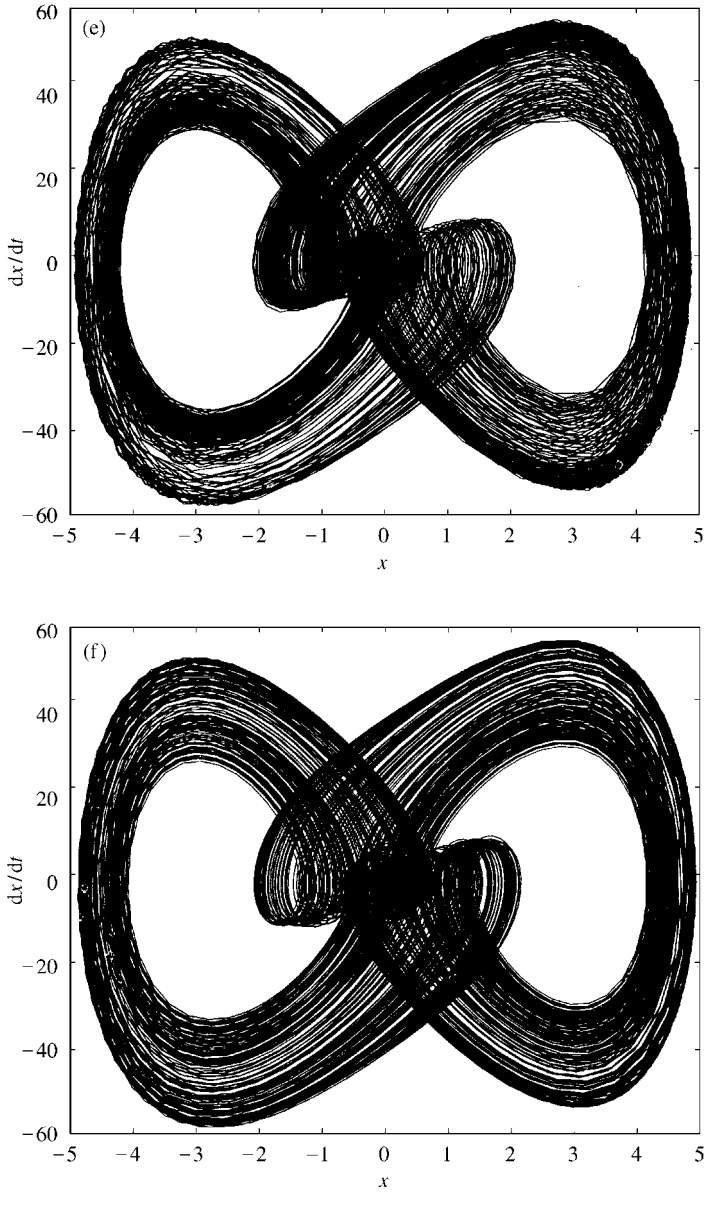

Figure 3. Continued.

coefficient β can be well approximated by a constant. Such an observation may probably be used as an alternative characterization for chaotic orbits, but is not touched upon here.

4. PATHWISE STOCHASTIC LINEARIZATION

Here it will be convenient to start with a class of s.d.o.f. oscillators straight away, keeping in mind that the arguments are readily extendible to m.d.o.f. oscillators.

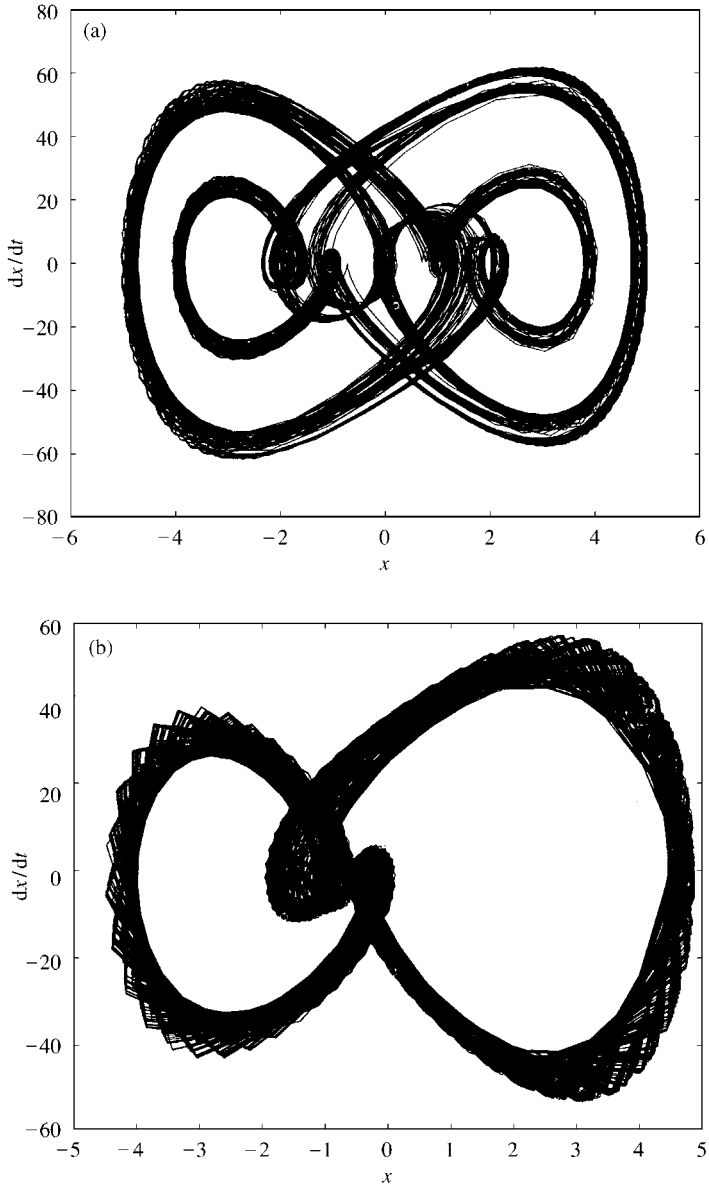

Figure 4. Effect of time step size on the chaotic orbit. (a) Two terms in the averaged Taylor's expansion, $h = 0{\cdot}01$, (g) simulation by Runge–Kutta (sixth order) scheme, $h = 0{\cdot}01$.

Thus, the class of two-dimensional stochastic differential equations considered are given by

$$\ddot{x} + 2\pi\varepsilon_1\dot{x} + 4\pi^2\varepsilon_2 g(x)x = 4\pi^2\varepsilon_3\cos(2\pi t) + \sigma(t)\xi(t), \tag{29}$$

where $\sigma(t) \in L^2([0, +\infty), B([0, t]), \mu)$, $t \geqslant 0$ denotes, in a sense, the strength of the white noise $\xi(t)$ which is in turn defined formally as $\xi(t) = \mathrm{d}W(t)/\mathrm{d}t$, and $W(t)$ is

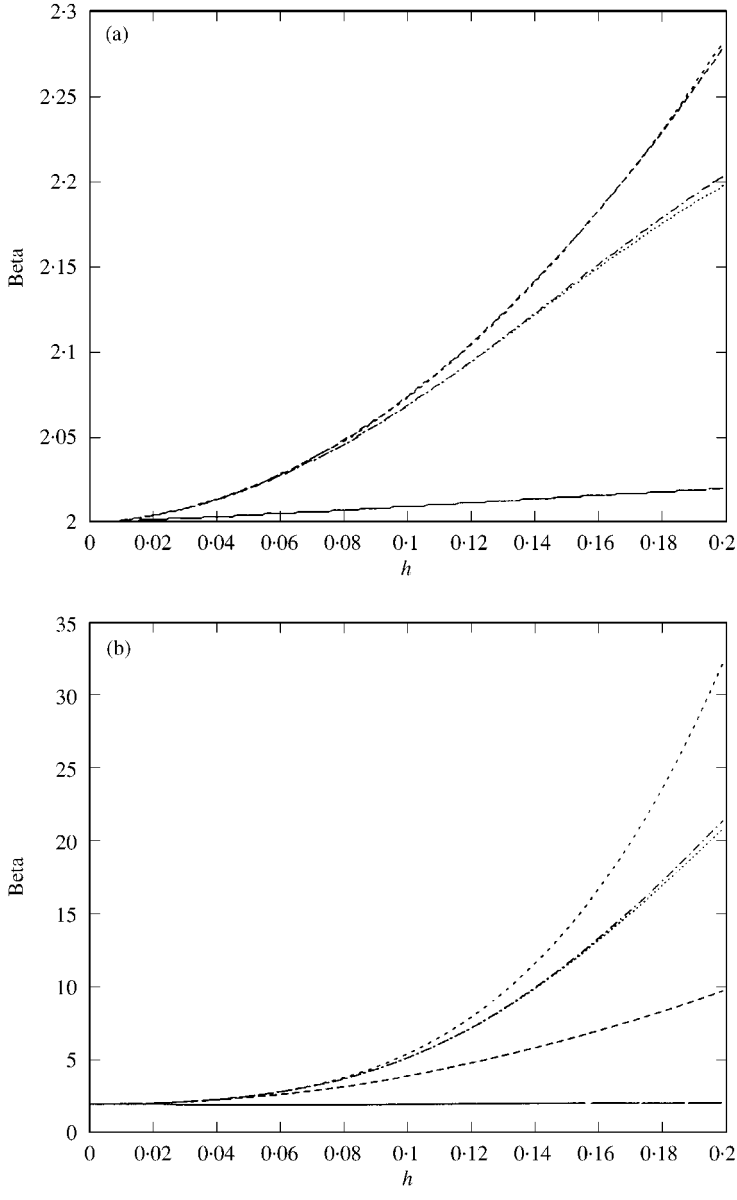

Figure 5. Effect of the time step size on the parameter β. (a) periodic regime, $\varepsilon_1 = 0{\cdot}25$, $\varepsilon_2 = 0{\cdot}5$, $\varepsilon_3 = 1$, $x_0 = 1$, $\dot{x}_0 = 0{\cdot}1$, (b) chaotic regime, $\varepsilon_1 = 0{\cdot}25$, $\varepsilon_2 = 0{\cdot}51$, $\varepsilon_3 = 15{\cdot}3$, $x_0 = 1$, $\dot{x}_0 = 0{\cdot}1$: STL : $N = 2$ ——; STL : $N = 3$ – – – –; STL : $N = 4$ - - - - -; STL : $N = 5$ ·····; STL : $N = 6$ –·–· .

a Wiener process with independent Gaussian increments. The above SDE may conveniently be recast in the following form:

$$\begin{aligned} \mathrm{d}x_1(t) &= x_2(t)\,\mathrm{d}t = a_1(x_1, x_2, t)\,\mathrm{d}t \\ \mathrm{d}x_2(t) &= \{-2\pi\varepsilon_1 x_2 - 4\pi^2\varepsilon_2 g(x_1)x_1 + 4\pi^2\varepsilon_3 \cos(2\pi t)\}\,\mathrm{d}t + \sigma(t)\,\mathrm{d}W(t) \\ &= a_2(x_1, x_2, t)\,\mathrm{d}t + \sigma(t)\,\mathrm{d}W(t). \end{aligned} \tag{30}$$

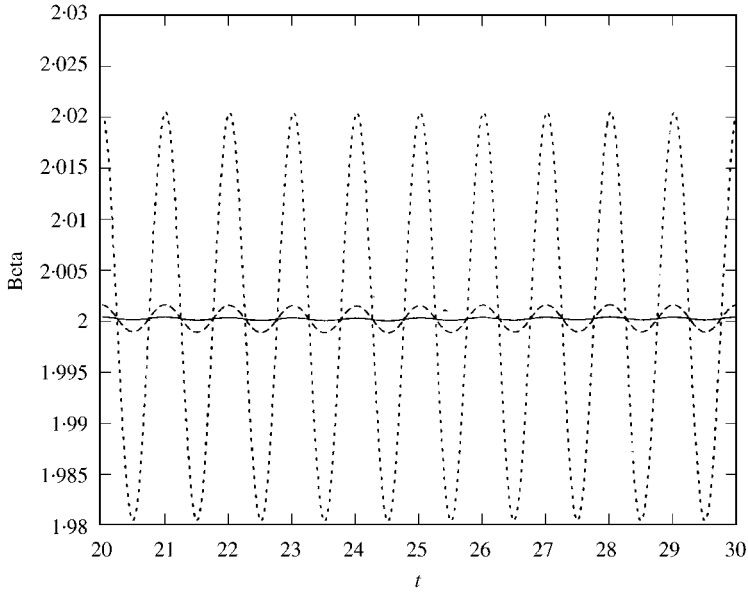

Figure 6. Evolution of the parameter β with time, periodic and chaotic regimes; ——, Small 1-periodic orbit, $\varepsilon_1 = 0{\cdot}25$, $\varepsilon_2 = 0{\cdot}5$, $\varepsilon_3 = 0{\cdot}1$, – – – –, large 1-periodic orbit, $\varepsilon_1 = 0{\cdot}25$, $\varepsilon_2 = 0{\cdot}5$, $\varepsilon_1 = 1$, $\cdots$, chaotic orbit, $\varepsilon_1 = 0{\cdot}25$, $\varepsilon_2 = 0{\cdot}51$, $\varepsilon_3 = 15{\cdot}3$.

The above equation reduces to the Duffing oscillator for $g(x) = 1 + x^2$. Given the same ordering of the time axis as before, the essence of the idea is to find out a set of conditionally linear SDEs or equivalently a set of conditionally Gaussian TPDs at time $t = t_{i+1}$, given the points in the state space at the immediately preceding time

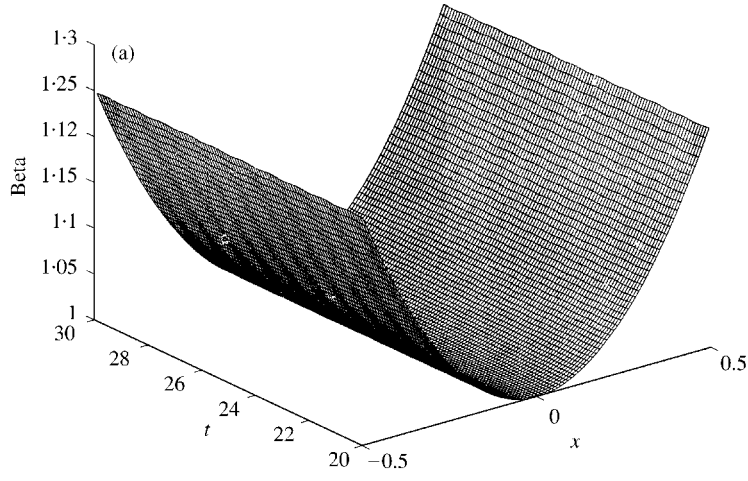

Figure 7. Three-dimensional surface plots for the parameter β with time (periodic and chaotic regimes): (a) plot $\beta - x_i - t_i$, periodic regime, $\varepsilon_1 = 0{\cdot}25$, $\varepsilon_2 = 0{\cdot}5$, $\varepsilon_3 = 1$, $\dot{x}_0 = 0{\cdot}1$, (b) plot $\beta - x_i - t_i$, chaotic regime, $\varepsilon_1 = 0{\cdot}25$, $\varepsilon_2 = 0{\cdot}51$, $\varepsilon_3 = 15{\cdot}3$, $\dot{x}_0 = 0{\cdot}1$, (c) plot $\beta - \dot{x}_i - t_i$, periodic regime, $\varepsilon_1 = 0{\cdot}25$, $\varepsilon_2 = 0{\cdot}5$, $\varepsilon_3 = 1$, $x_0 = 0$, (d) plot $\beta - \dot{x}_i - t_i$, chaotic regime, $\varepsilon_1 = 0{\cdot}25$, $\varepsilon_2 = 0{\cdot}51$, $\varepsilon_3 = 15{\cdot}3$, $x_0 = 1$.

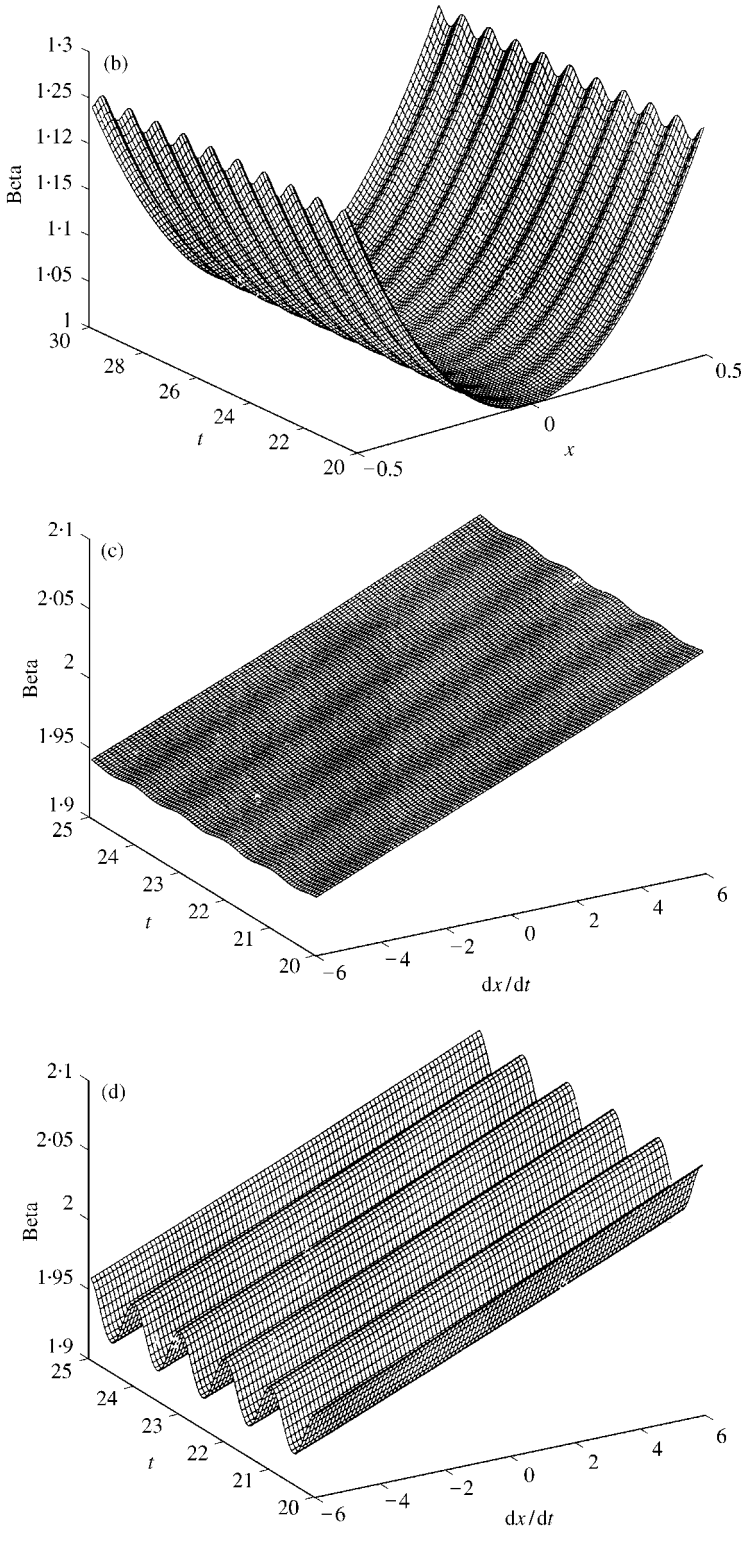

Figure 7. Continued.

instant on the ordered axis, i.e., $t = t_i$. Towards this end, one way is to suitably linearize the state-dependent *non-linearity coefficient* $g(x)$ over the semi-closed interval T_1. To begin with, let $\exists C > 0$ such that $\int_R g(x)\,\mathrm{d}x$ exists, is bounded below by

$$\int_0^x g(\psi)\,\mathrm{d}\psi \geqslant -C(1 - x^2) \tag{31}$$

and is finite. It is now intended to replace $g(x)$ by a real constant over T_i such that the resulting SDE is linear with constant coefficients in T_i. Towards this, $g(x)$ is first expanded into an Ito–Taylor (alternatively called Wagner–Platen) series [8] as follows:

$$g(x_1(t)) = g(x_1(t_i)) + \int_{t_i}^t L^{(0)}g(x_1(\psi))\,\mathrm{d}\psi + \int_{t_i}^t L^{(1)}g(x_1(\psi))\,\mathrm{d}\psi, \quad t \in T_i. \tag{32}$$

The operators, $L^{(0)}$ and $L^{(1)}$ are defined as

$$\begin{aligned} L^{(0)}g(x_1) &= \left(\frac{\partial}{\partial t} + x_2\frac{\partial}{\partial x_1} + a_2(t, x_1, x_2)\frac{\partial}{\partial x_2} + 0{\cdot}5\sigma^2(t)\frac{\partial^2}{\partial x_2^2}\right)g(x_1) \\ &= x_2 g'(x_1), \\ L^{(1)}g(x_1) &= \left(\sigma(t)\frac{\partial}{\partial x_2}\right)g(x_1) = 0, \end{aligned} \tag{33}$$

where $g'(x_1) = (\partial/\partial x_1)g(x_1)$. Now $g'(x_1)$ is expanded as

$$\begin{aligned} g'(x_1(t)) &= g(x_1(t_i)) + \int_{t_i}^t x_2(\psi)g'(x_1(\psi))\,\mathrm{d}\psi \\ &= g(x_1(t_1)) + x_2(t_i)g'(x_1(t_i))\Delta t + \int_{t_i}^t \left[\int_{t_i}^{\psi} x_2^2(\psi)g''(x_1(\psi))\right. \\ &\quad \left. + a_2(s, x_1(s), x_2(s))g'(x_1(s))\,\mathrm{d}s\right]\mathrm{d}\psi \\ &\quad + \int_{t_i}^t \int_{t_i}^{\psi} \sigma(u)g'(x_1(u))\,\mathrm{d}W_u\,\mathrm{d}\psi. \end{aligned} \tag{34}$$

Expanding the terms of only the lowest order, i.e., $\int_{t_i}^{t}\int_{t_i}^{\psi}\sigma(u)g'(x_1(u))\,\mathrm{d}W_u\,\mathrm{d}\psi$, one gets

$$\int_{t_i}^{t}\int_{t_i}^{\psi}\sigma(u)g'(x_1(u))\,\mathrm{d}W_u\,\mathrm{d}\psi = \sigma(t_i)g'(x_1(t_i))\int_{t_i}^{t}\int_{t_i}^{\psi}\mathrm{d}W_u\,\mathrm{d}\psi + \int_{t_i}^{t}\int_{t_i}^{\psi}\int_{t_i}^{u}[\sigma'(v)g'(x_1(v)) + \sigma(v)x_2(v)g''(x_1(v))]\,\mathrm{d}v\,\mathrm{d}W_u\,\mathrm{d}\psi + \int_{t_i}^{t}\int_{t_i}^{\psi}\int_{t_i}^{u}\sigma(t)\frac{\partial}{\partial x_2}(\sigma(t)g'(x_1(u))\,\mathrm{d}W_v\,\mathrm{d}W_u\,\mathrm{d}\psi. \quad (35)$$

Now, for the Duffing oscillator, the function g is independent of x_2 and hence the third term of the right-hand side of the above equation vanishes. Thus to an approximation of $O(h_i)$, one has

$$g(x_1(t)) \cong g(x_1(t_i)) + x_2(t_i)g'(x_1(t_i))\Delta_t \quad (36)$$

which is identical to a deterministic Taylor expansion. On the other hand, if one continues to hierarchically expand and functional g, then $O(h_i^{1\cdot 5})$ approximation yields

$$g(x_1(t)) \cong g(x_1(t_i)) + x_2(t_i)g'(x_1(t_i))\Delta_t + \sigma(t_i)g'(x_1(t_i))\int_{t_1}^{t}\int_{t_i}^{\psi}\mathrm{d}W_u\,\mathrm{d}\psi, \quad (37)$$

where the double integral in the third term on the right-hand side of the above equation reduces to

$$\int_{t_1}^{t}\int_{t_i}^{\psi}\mathrm{d}W_u\,\mathrm{d}\psi = \int_{t_1}^{t}(W(s) - W(t_i))\,\mathrm{d}s = I_{(0,1)\Delta_t}, \quad (38)$$

where $I_{(0,1)\Delta_t}$ denotes the multiple stochastic integral (see Appendix A) following Kloeden and Platen [8]. Similarly, to an approximation of $O(h_i^2)$, one has

$$g(x_1(t)) \cong g(x_1(t_i)) + x_2(t_i)g'(x_1(t_i))\Delta_t + \sigma(t_i)g'(x_1(t_i))I_{(0,1)\Delta_t} + [x_2^2(t_i)g''(x_1(t)) + a_2(t_i, x_1(t_i), x_2(t_i))g'(x_1(t_i))]\frac{\Delta_i^2}{2}. \quad (39)$$

In this way, one can, in principle, proceed with the Ito–Taylor approximation to include higher order terms in the series and, thus, in the interval I, one finally has

$$g(x_1) = \sum_{\alpha\in A_\Gamma} g_\alpha(t_i, x_1(t_i), x_2(t_i))I_{\alpha,\Delta_t} + \sum_{\alpha\in\Re(A_\Gamma)} g_\alpha(t_i, x_1(t_i), x_2(t_i))I_{\alpha,\Delta_t}, \quad (40)$$

where A_Γ and $\Re(A_\Gamma)$ are, respectively, the hierarchical and residual sets of the Ito–Taylor expansion (see Appendix A1) and $\Gamma \in \{\frac{1}{2}, 1, \frac{3}{2}, 2, \dots\}$ may be considered to be the "order of linearization". Moreover g_α and I_{α, Δ_t} are, respectively, the Ito coefficient functions and multiple Ito integrals (see Appendix AI) [8]. Now, in order to make the linearized vector field strictly time invariant, $g(x_1)$ is replaced over I by the following short-time-averaged form:

$$g(x_1) = \beta(x_1, t_i, h_i) = \frac{1}{h_i} \int_{t_i}^{t_i + h_i} \sum_{\alpha \in A_\Gamma} g_\alpha(t_i, x_1(t_i), x_2(t_i)) I_{\alpha, \Delta_t} \, \mathrm{d}s, \tag{41}$$

where

$$\Delta_z = s - t_i, \; t_{i+1} \geqslant s \geqslant t_i. \tag{42}$$

Thus, over the interval I, one can replace the non-linear SDE, as in equation (35), by the conditionally linear SDE given by

$$\ddot{y} + 2\pi\varepsilon_1 \dot{y} + 4\pi^2 \varepsilon_2 \beta(x_i, \dot{x}_i, t_i, h_i) y = 4\pi^2 \varepsilon_3 \cos(2\pi t) + \sigma(t)\xi(t). \tag{43}$$

Here it may be pointed out that a similar approach based on a Stratonovich–Taylor expansion is also possible and will lead to different results only when the stochastic excitation is multiplicative. Here, considering an additive case, if $g(x_1) = 1 + x_1^2$ and $\sigma(t) = \sigma = \pi G_0$, the twin operations of Ito–Taylor (or Ito–Stratonovich) expansion followed by short-time averaging on $g(x_1)$ lead to the following expression for β in I:

$$\beta = g(x_1(t_i)) + x_1(t_i) x_2(t_i) h_i + \frac{2}{h_i} \pi G_0 x_1(t_i) \int_{t_i}^{t_i + h} \left\{ \int_{t_i}^{t} W_s \, \mathrm{d}s \right\} \mathrm{d}t$$

$$+ \frac{1}{3} \{ x_2^2(t_i) - 2\pi\varepsilon_1 x_1(t_i) x_2(t_i) - 4\pi^2 \varepsilon_2 x_1^4(t_i) + 4\pi^2 \varepsilon_3 x_1(t_i) \cos(2\pi t_i) \} h_i^2 + O(h_i^{2 \cdot 5}). \tag{44}$$

A careful inspection of the above equation reveals the effect of stochasticity on the present linearization procedure. In particular, the third term on the RHS of the above expression is the crucial term that may be considered to be a higher order stochastic correction term, the never comes into play in a purely deterministic Taylor expansion. This basic technique of linearizing a non-linear SDE via a stochastic Taylor expansion followed by a short-time averaging would henceforth be referred to as "pathwise stochastic linearization" (PSL). The conditionally linear SDEs are given by equation (43) may now be exploited for establishing certain semi-analytical tools for a quantitative analysis of the non-linear stochastic flow. In what follows, a couple of such tools are detailed.

4.1. SIMULATION USING PSL AND A HALF-DRIFT-IMPLICIT METHOD

As has already been indicated, SDE (43) may be treated as conditionally linear over the interval $I = [t_i, t_{i+1})$, given the "sharp" values of the state variables $\{x_i, \dot{x}_i\}$ at the left closed end, t_i. Thus, each of the approximating state variables $\{{}^j y(t), {}^j\dot{y}(t) | \, j = 1, 2, \ldots, N_s, t \in I\}$, N_s being the number of samples in the ensemble, may be represented as ${}^j y = {}^j x | {}^j x_i$ and ${}^j\dot{y} = {}^j\dot{x} | {}^j\dot{x}_i$. Now it is convenient to introduce the following decomposition in I and $\forall j \in \{1, 2, \ldots, N_s\}$, $i \in \{1, 2, 3, \ldots\}$:

$$ {}^j y(t) = {}^j m(t) + {}^j z(t), \qquad {}^j\dot{y}(t) = {}^j\dot{m}(t) + {}^j\dot{z}(t) \tag{45} $$

so that

$$ {}^j m(t) = \langle {}^j x(t) | {}^j x_i \rangle, \qquad {}^j\dot{m}(t) = \langle {}^j\dot{x}(t) | {}^j\dot{x}_i \rangle, $$

$$ \langle {}^j z(t) \rangle = \langle {}^j\dot{z}(t) \rangle = {}^j z_i = {}^j\dot{z}_i = 0. \tag{46} $$

This results in the following pair of second order differential equations in the conditional quantities, ${}^j m$ and ${}^j z$:

$$ {}^j\ddot{m} + 2\pi\varepsilon_1 {}^j\dot{m} + 4\pi^2\varepsilon_2\beta {}^j m = 4\pi^2\varepsilon_3 \cos(2\pi t), $$

$$ {}^j\ddot{z} + 2\pi\varepsilon_1 {}^j\dot{z} + 4\pi^2\varepsilon_2\beta {}^j z = \dot{W}(t), \quad t \in I. \tag{47} $$

Conditioned on the deterministic choice of $\{{}^j x_i, {}^j\dot{x}_i\}$, the first of the above pair of equations is a purely deterministic ODE, while the second one is a linear SDE with zero initial conditions. In order to solve for this latter SDE, stochastic trapezoidal or the half-drift implicit method is made use of. Thus, one has

$$ {}^j z_{i+1} = {}^j z_i + \tfrac{1}{2}({}^j\dot{z}_i + {}^j\dot{z}_{i+1}) h_i, $$

$$ {}^j\dot{z}_{i+1} = {}^j\dot{z}_i + \tfrac{1}{2}(2\pi\varepsilon_1 {}^j\dot{z}_i + 4\pi^2\varepsilon_2\beta {}^j\dot{z}_{i+1}) h_i + \sqrt{\pi G_0 h_i}\,\xi_{i+1}, \tag{48} $$

where $\xi_{i+1} \in \mathrm{N}(0, 1)$ with the symbol N denoting normal distribution. At this stage, it is interesting to note that the use of zero initial conditions in equation (48) reduces the implicit half-drift scheme to an explicit one and leads to the following simple pair of equations:

$$ {}^j z_{i+1} = \tfrac{1}{2} {}^j z_{i+1} h_i, $$

$$ {}^j\dot{z}_{i+1} = \sqrt{\pi G_0 h_i}\,\xi_{i+1}/(1 + \pi\varepsilon_1 h_1 + \pi^2\varepsilon_2\beta h_i^2). \tag{49} $$

At each time instant along the ordered time axis, the above set of operations needs to be performed for every $j \in \{1, 2, \ldots, N_z\}$ and thus one can march forward in time to get the time history for the statistical moments as well as the evolving TPD.

Success of this scheme in obtaining useful results crucially depends on accurate generation of certain random quantities, namely $1/h_i \int_{t_1}^{t_{i+1}} \int_{t_i}^{t} W(s)\,\mathrm{d}s\,\mathrm{d}t$ and $\int_{t_1}^{t_{i+1}} \mathrm{d}W(s)$. These quantities are more conveniently written in terms of multiple stochastic integrals as

$$\frac{1}{h_i}\int_{t_1}^{t_{i+1}} \int_{t_i}^{t} W(s)\,\mathrm{d}s\,\mathrm{d}t = \frac{1}{h_i} I_{(0,0,1),t_i,t_{i+1}}, \quad \int_{t_i}^{t_{i+1}} \mathrm{d}W(s) = I_{(1),t_i,t_{i+1}}. \tag{50}$$

It is obvious that this pair of correlated random variables are jointly Gaussian with zero mean. It now remains to determine their covariance matrix. First, it is noted that

$$E(I^2_{(1),t_i,t_{i+1}}) = t_{i+1} - t_i = h_i. \tag{51}$$

Exploiting the fundamental relationship between Ito integrals, I_α and I_β, given by [8]

$$I_{\alpha,t} I_{\beta,t} = \int_{t_i}^{t} I_{\alpha,s} I_{\beta-,s}\,\mathrm{d}W_s^{ji(\beta)} + \int_{t_i}^{t} I_{\alpha-,s} I_{\beta,s}\,\mathrm{d}W_s^{jl(\alpha)}$$

$$+ I_{\{j_i(\alpha)=j_i(\beta)\neq 0\}} \int_{t_i}^{t} I_{\alpha-,s} I_{\beta-,s}\,\mathrm{d}s \tag{52}$$

one gets

$$\frac{1}{h_i^2} E(I^2_{(00,1),t_i,t_{i+1}}) = \frac{1}{6} h_i,$$

$$\frac{1}{h_i} E(I^2_{(1),t_i,t_{i+1}} I_{(0,0,1),t_i,t_{i+1}}) = \frac{1}{h_i} E(I_{(1),0,h_i} I_{(0,0,1),0,h_i}) = \frac{h_i^2}{6}, \tag{53}$$

where the symbol I in equation (52) denotes the usual indicator function. Thus, all the elements of the covariance matrix of the vector process $\{{}^j z_{i+1}, {}^j \dot{z}_{i+1}\}$ are now determined.

4.2. A SCHEME BASED ON FOKKER–PLANCK EQUATION APPROACH

The PSL technique described so far decomposes a given non-linear SDE a countable set of conditionally linear SDEs, each valid over a sufficiently small time interval on the suitably ordered time axis. Since the response of these conditionally linear SDEs under Gaussian inputs are Gaussian, it may be concluded that the conditional response of the non-linear, given the values of the state variables at the immediately preceding time instant, is Gaussian under Gaussian excitations and over a small time interval. This observation is not new

and is quite consistent with the expansion of the Fokker–Planck operator over a small time step, which leads to a conditionally Gaussian distribution for the evolving TPD [11]. These conditionally Gaussian TPDs can be readily generated within the framework of the PSL scheme, making use of the well-known theory of linear random vibration. These TPDs may then be used for generating random state variables at the current time instant. In order to generate these TPDs, the same decomposition as in equations (45) and (46) are used, leading, as before, to equations (47) in conditional mean and random perturbation, ${}^{j}m$ and ${}^{j}z$ respectively. The ODE in ${}^{j}m$, being deterministic and linear, can be solved analytically. Moreover, the stochastic variation ${}^{j}z$ is Gaussian with zero mean. It only remains to obtain the non-stationary covariance matrix of the pair process ${}^{j}\bar{z} = \{{}^{j}z, {}^{j}\dot{z}\}$. This may be conveniently done by solving the associated Fokker–Planck equation in the non-stationary regime by the Fourier transform method [16]. The drift coefficients $\bar{p} = \{p_i, i = 1, 2\}$ and diffusion coefficients $\bar{q} = \{q_{i,j}, i, j = 1, 2\}$ corresponding to the second of equations (47) valid over $t \in [t_i, t_{i+1})$ are given by

$$p_1 = {}^{j}\dot{z}, \qquad p_2 = -4\pi^2\varepsilon_2\beta\,{}^{j}z - 2\pi\varepsilon_1\,{}^{j}\dot{z}, \qquad q_{11} = q_{12} = q_{21} = 0, \qquad q_{22} = \pi G_0, \tag{54}$$

Equivalently,

$$\bar{p} = T({}^{j}\bar{z}). \tag{55}$$

The two eigenvalues associated with the conditional endomorphism T are

$$\begin{aligned} \lambda_{1,2} &= \pi\varepsilon_1 \pm \pi\sqrt{\varepsilon_1^2 - 4\varepsilon_2\beta} \quad \text{if } \varepsilon_1^2 > 4\varepsilon_2\beta \\ &= \pi\varepsilon_1 \pm k\pi\sqrt{\varepsilon_1^2 - 4\varepsilon_2\beta} \quad \text{if } \varepsilon_1^2 > 4\varepsilon_2\beta, \end{aligned} \tag{56}$$

where $k = \sqrt{-1}$. Now ${}^{j}\bar{z}(t)$ is linearly transformed to ${}^{j}\bar{r}(t)$ so that

$${}^{j}\bar{r}(t) = [C]\,{}^{j}z(t) \tag{57}$$

with

$$[C]\,T\,[C]^{-1} = \operatorname{diag}\{\lambda_1 \;\; \lambda_2\}. \tag{58}$$

The elements of the matrix $[C]$ can be readily found from the eigenvectors of T. Now in terms of the transformed vector process ${}^{j}\bar{r}(t)$ the diffusion coefficients v_{ij} may be found as

$$[v_{ij}] = [C][P][C]^{\mathrm{T}}, \tag{59}$$

where the elements of the matrix $[P]$ are given by

$$p_{11} = p_{12} = p_{21} = 0, \qquad p_{22} = \pi G_0. \tag{60}$$

The conditional TPD $p({}^j\bar{r}(t)|{}^j\bar{r}(t_i))$ is bivariate Gaussian with the mean vector

$$m_{j_{r(t)}} = {}^jr(t_i)\exp(\lambda_1 t), \qquad m_{j_{\dot{r}(t)}} = {}^j\dot{r}(t_i)\exp(\lambda_2 t) \tag{61}$$

and the covariance matrix

$${}^{\bar{r}}\Gamma_{ij}(t) = \left[\frac{-v_{ij}}{\lambda_i + \lambda_j}\{1 - \exp(\lambda_i + \lambda_j)(t - t_i)\}\right]. \tag{62}$$

At this stage the mean and covariance matrices of the bivariate Gaussian process ${}^j\bar{z}(t)$ may be extracted as

$$\bar{m}_{\bar{z}}(t) = [C]^{-1}\bar{m}_{\bar{r}}(t), \qquad {}^{\bar{z}}\Gamma(t) = [C]^{-1}[{}^{\bar{r}}\Gamma(t)][C^{-1}]^{\mathrm{T}}. \tag{63}$$

Thus, the conditionally Gaussian local distribution of the evolving flow is completely defined.

The following set of operations may be used for a fast stochastic simulation of a given SDE. The phase space is first represented discretely at $t = t_i$ by a finite number of points ${}^j\bar{x}_i = \{{}^jx_i, {}^j\dot{x}_i | j = 1, 2, \ldots, N_z, \ i \in \{1, 2, \ldots, \infty\}\}$, and corresponding to every such point the methodology as outlined above may be used for generating the bivariate (multivariate in case of systems of dimension greater than 2) and zero-mean conditionally Gaussian TPD over a given short time step. Standard schemes, such as Box–Muller or Polar–Marsaglia methods [ ] may be used for generating the independent and zero-mean Gaussian random variables $\{{}^jG_1, {}^jG_2\}$. The state variables $\{{}^jx_{i+1}, {}^j\dot{x}_{i+1}\}$ may now be obtained as

$${}^jx_{i+1} = {}^jm_{i+1} + w_0\,{}^jG_1, \qquad {}^j\dot{x}_{i+1} = {}^jx_{i+1} + w_1\,{}^jG_1 + w_2\,{}^jG_2, \tag{64}$$

where ${}^jm_{i+1}$ and ${}^j\dot{m}_{i+1}$ are found by analytically solving the mean equation (first of equations (47)) and w_0, w_1, w_2 are real numbers calculated from

$$w_0 = \sqrt{{}^jz\Gamma_{11}(t_{i+1})}, \qquad w_1 = \frac{{}^jz\Gamma_{12}(t_{i+1})}{\sqrt{{}^jz\Gamma_{11}(t_{i+1})}}, \qquad w_2 = \sqrt{w_0^2 - w_1^2}, \tag{65}$$

starting with $t = t_0$, i.e., the initial time the above set of operations may be carried out repeatedly to move forward in time.

Here it is worth noting that a somewhat similar procedure as outlined in this subsection has been tried out by Askar *et al.* [10] wherein the drift coefficients have been linearized using different moving averaging techniques, which allowed the construction of the conditionally Gaussian distribution. However, the present method is believed to be more accurate due to a better approximation of the sample paths.

4.3. NUMERICAL RESULTS

A few numerical results obtained for a class of non-linear SDOF oscillators will be presented here to illustrate the schemes outlined in sections 4.1 and 4.2. Extension to non-linear m.d.o.f. oscillators should present no further difficulties than more elaborate algebraic manipulations. The hardening Duffing oscillator (equation (35)) with $g(x) = 1 + x^2$ and $\sigma(t) = \sqrt{\pi G_0}$ is taken up for further considerations. It may be pointed out here that under purely stochastic excitation, i.e., $\varepsilon_3 = 0$, there is a stationary solution for the associated (reduced) Fokker–Planck equation. The analytical expression for this TPD is available in closed form and is given by

$$p(x, \dot{x}) = D \exp\left(-\frac{4\pi^2 \varepsilon_1 \varepsilon_2}{G_0}(x^4 + 2x^2) - \frac{2\varepsilon_1}{G_0}\dot{x}^2 \right), \tag{66}$$

where D is a normalization constant and has the form

$$D = \frac{1}{\int_{-\infty}^{\infty} \exp\left(-\frac{4\pi^2 \varepsilon_1 \varepsilon_2}{G_0}(x^4 + 2x^2) \right) \mathrm{d}x \int_{-\infty}^{\infty} \exp\left(\frac{2\varepsilon_1}{G_0}\dot{x}^2 \right) \mathrm{d}\dot{x}}. \tag{67}$$

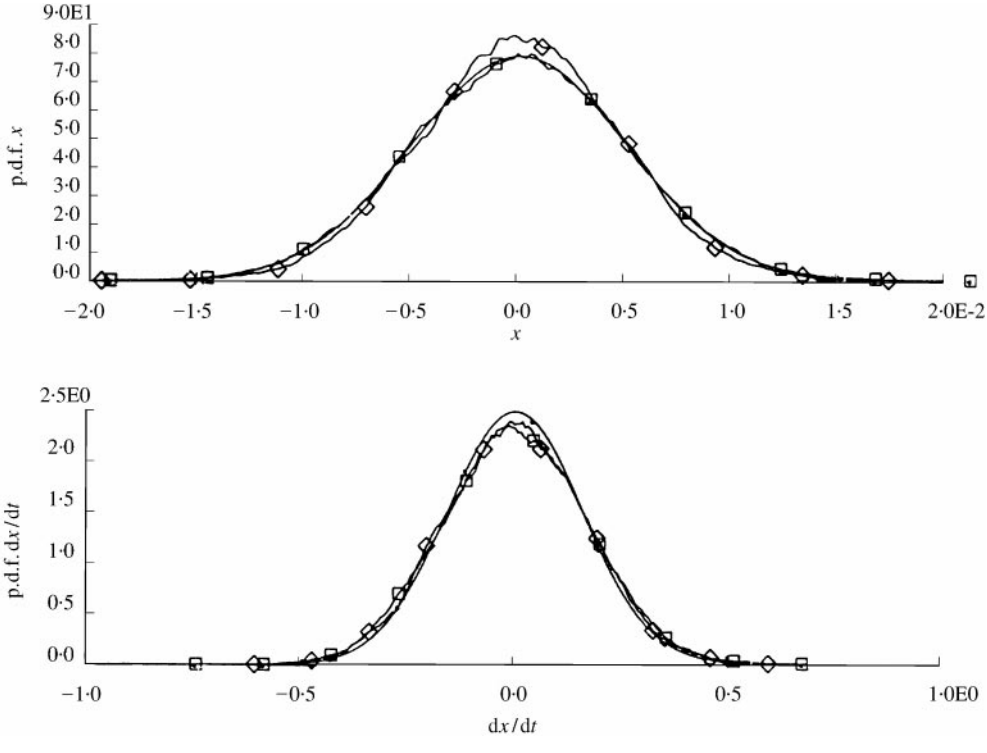

Figure 8. Stationary TPD for the Duffing oscillator under white noise excitation: (a) process $x(t)$, (b) process $\dot{x}(t)$. ◇ fast_MCS; □ half_drift; e. exact.

It may be observed that the above non-Gaussian stationary distribution has zero mean, and so is reflected in Figure 8 where the stationary TPDs of the displacement and velocity processes are shown using both PSL with the half-drift implicit scheme (henceforth called method 1) and the simulation scheme of section 4.2 (henceforth called method 2). In the same figure, these stationary TPDs are compared with the corresponding exact stationary TPDs as given by equations (66) and (67). The comparison seems to be very good especially so for method 1 and for a reasonably high sample size ($N_z = 10\,000$ onwards). In case $\varepsilon_3 \neq 0$ and $G_0 = 0$, i.e., the oscillator is deterministically forced, it is well known that multiperiodic as well as chaotic response is possible. For example, a period 3 orbit is shown in Figure 9(a) using the deterministic version of the piecewise linearization procedure as outlined in section 3.3. It is now of interest to see the effect of a stochastic perturbation in the form of a weak white noise on the three periodic orbit. Thus the corresponding non-stationary TPD at time $t = 50$ s is shown in Figure 9(b) using method 2, 16 000 samples and a time step of 0·01. The TPD is distinctly multimodal with three conspicuous peaks. In Figure 3, a chaotic orbit with $G_0 = 0$ and in Figure 10, the corresponding TPD with $G_0 = 0{\cdot}1$ are shown. Even though the non-stationary nature of the TPD is clear enough, no discernible multimodal structure can be associated with this. It is of interest to observe that deterministic chaos in the hardening Duffing oscillator does not take place via a series of homoclinic bifurcations route, and thus it is expected that an addition of random noise of sufficiently weak intensity is unlikely to disturb the strange attractor, at least over a certain parameter range. This rather superficial observation is verified in

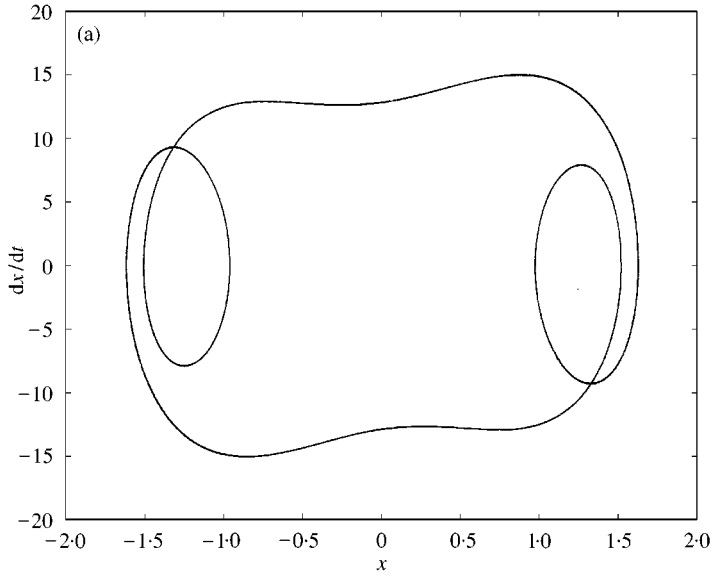

Figure 9. Effect of white noise on a typical 3-periodic orbit of the Duffing oscillator, $\varepsilon_1 = 0{\cdot}25$, $\varepsilon_2 = 3$, $\varepsilon_3 = 11{\cdot}1$. (a) deterministic 3-periodic orbit, (b) non-stationary TPD under combined deterministic forcing and weak white noise, $G_0 = 0{\cdot}1$.

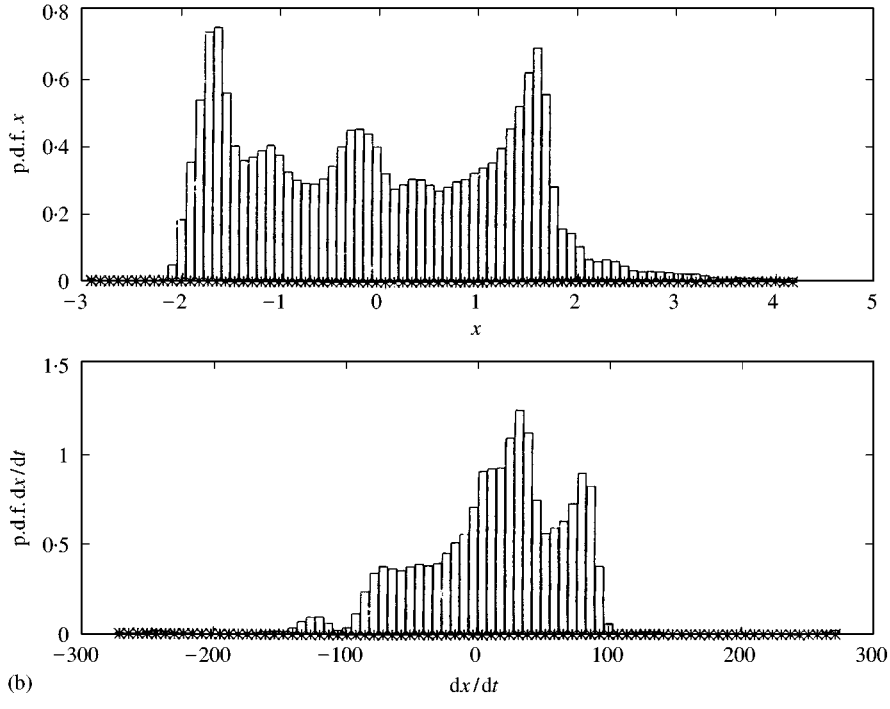

Figure 9. Continued.

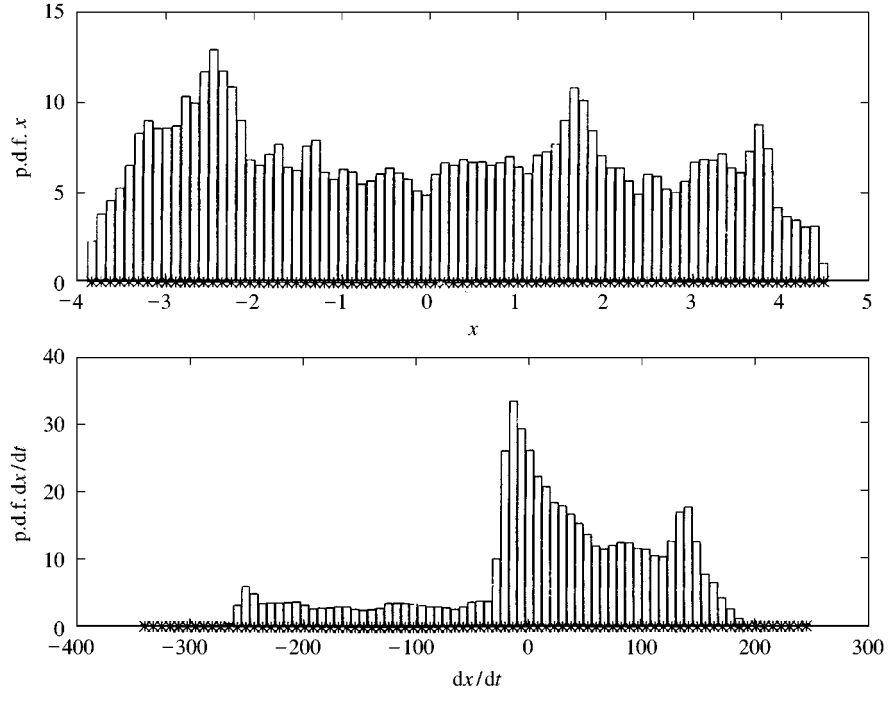

Figure 10. Effect of white noise on a typical chaotic orbit of the Duffing oscillator, $\varepsilon_1 = 0{\cdot}2$, $\varepsilon_2 = 0{\cdot}51$, $\varepsilon_3 = 15{\cdot}3$, $G_0 = 0{\cdot}1$.

Figure 11(a) where the phase plot of mean and its derivative is shown. This observation is further supported in Figures 11(b) and 11(c) where the evolutions of mean and variance functions are plotted with time. Curiously enough, it may be observed that after a certain time interval, the variances of both $x(t)$ and $\dot{x}(t)$ jump up, thereby confirming the exponential separation of nearby trajectories, as in the case of deterministic chaos [17]. Even more interesting is the case shown in

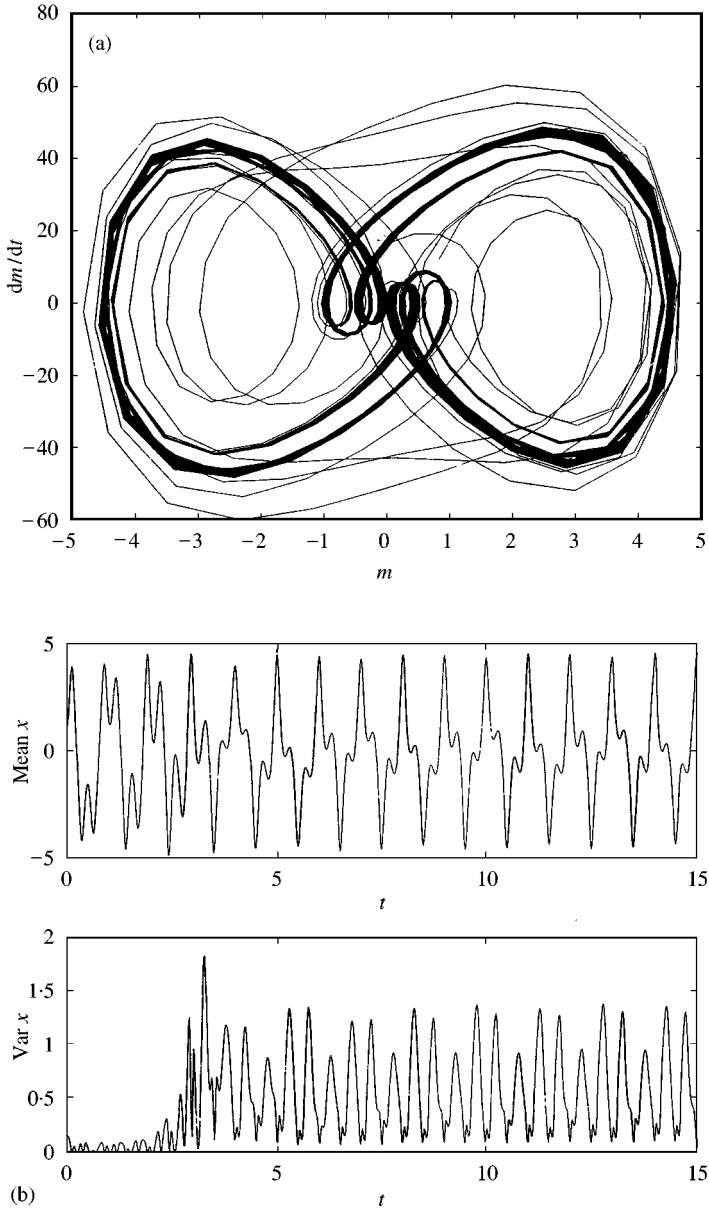

Figure 11. Persistence of the strange attractor under weak white noise, $\varepsilon_1 = 0{\cdot}2$, $\varepsilon_2 = 0{\cdot}51$, $\varepsilon_3 = 15{\cdot}3$, $G_0 = 0{\cdot}1$: (a) the phase plot of mean and its derivative, (b) evolutions of mean and variance of the process $x(t)$, (c) evolution of mean and variance of the process $\dot{x}(t)$.

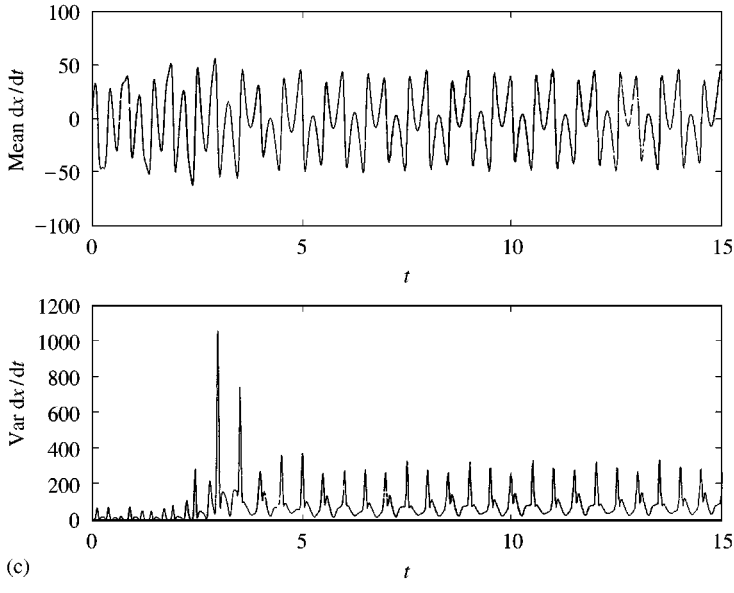

Figure 11. Continued.

Figures 12(a)–12(c) with a very high noise intensity, namely, $G_0 = 3{\cdot}0$. Even in such a case, the essential characteristics of a stochastic version of chaos, similar to Figures 11(a)–11(c), are visible. Chaos in this oscillator is generic in some sense. On the other hand, for ranges of parameters corresponding to periodic cases only

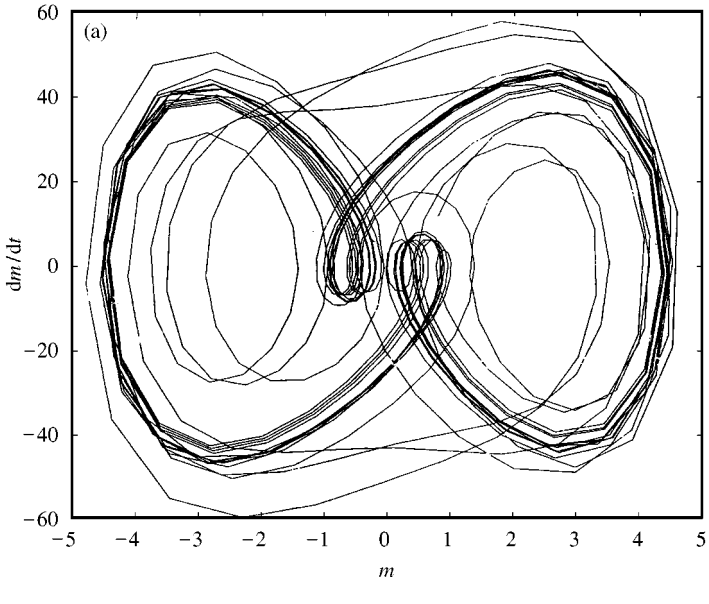

Figure 12. Persistence of the strange attractor under strong white noise, $\varepsilon_1 = 0{\cdot}2$, $\varepsilon_2 = 0{\cdot}51$, $\varepsilon_3 = 15{\cdot}3$, $G_0 = 3{\cdot}0$: (a) the phase plot of mean and its derivative, (b) evolutions of mean and variance of the process $x(t)$, (c) evolution of mean and variance of the process $\dot{x}(t)$.

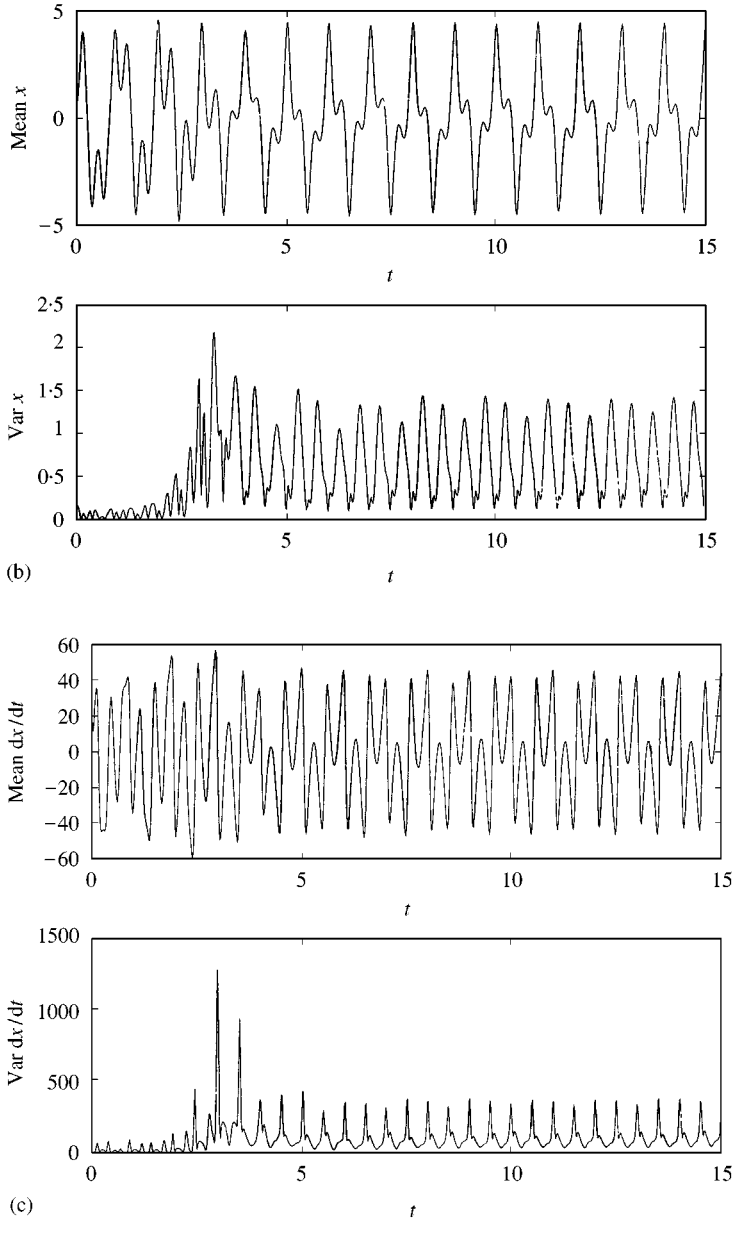

Figure 12. Continued.

under deterministic forcing, addition of noise does not generally lead to any qualitative change in the response scenario. This is observed in Figure 13(a) where the existence of the hyperbolically stable focus in the m–$\dot{m}$ plane is visible and in Figures 13(b) and 13(c) where no jumps in variances are observable, as expected.

5. DISCUSSION AND CONCLUSIONS

A novel linearization procedure for deterministic and stochastic non-linear engineering systems has been proposed here for semi-analytical simulations. The procedure outlined in this paper marks a sharp deviation from the standard equivalent linearization scheme (EQL) [18] in that the present method claims to accurately preserve even the most complicated topological characteristics in deterministic or stochastic response of these systems. Thus, in case of deterministic

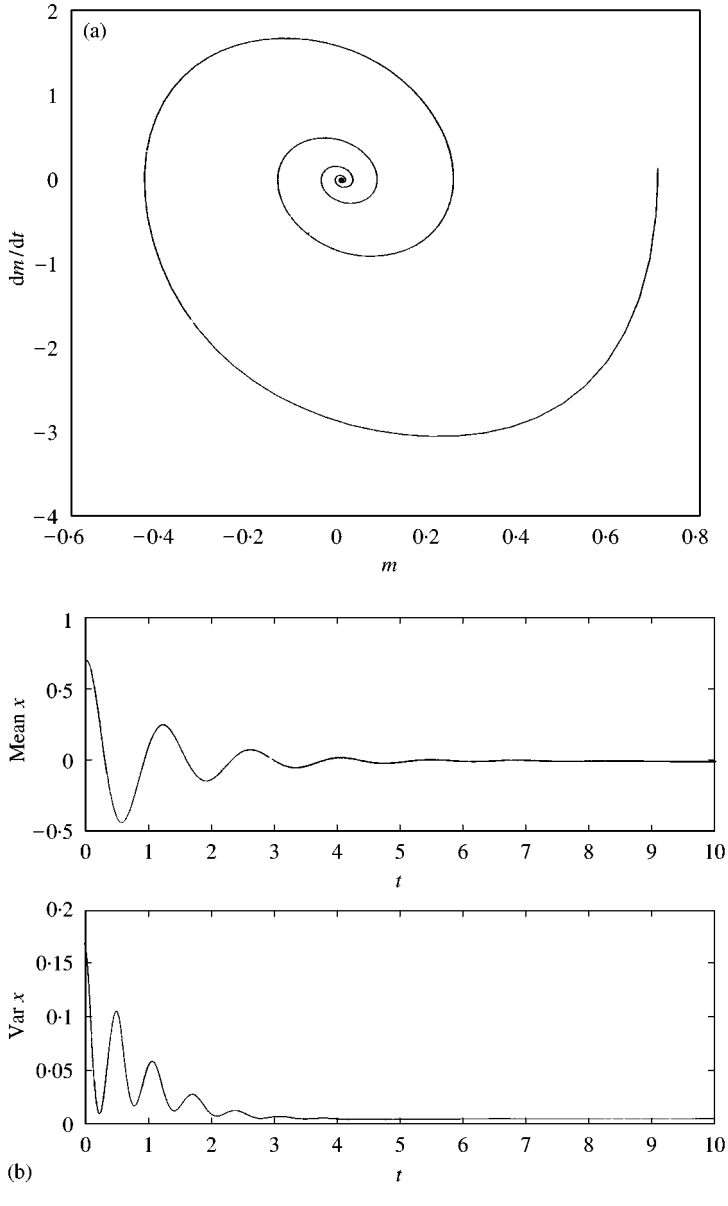

Figure 13. Persistence of the hyperbolically stable focus under white noise, $\varepsilon_1 = 0{\cdot}2$, $\varepsilon_2 = 0{\cdot}5$, $\varepsilon_3 = 0{\cdot}0$, $G_0 = 0{\cdot}1$: (a) the phase plot of mean and its derivative, (b) evolutions of mean and variance of the process $x(t)$, (c) evolution of mean and variance of the process $\dot{x}(t)$.

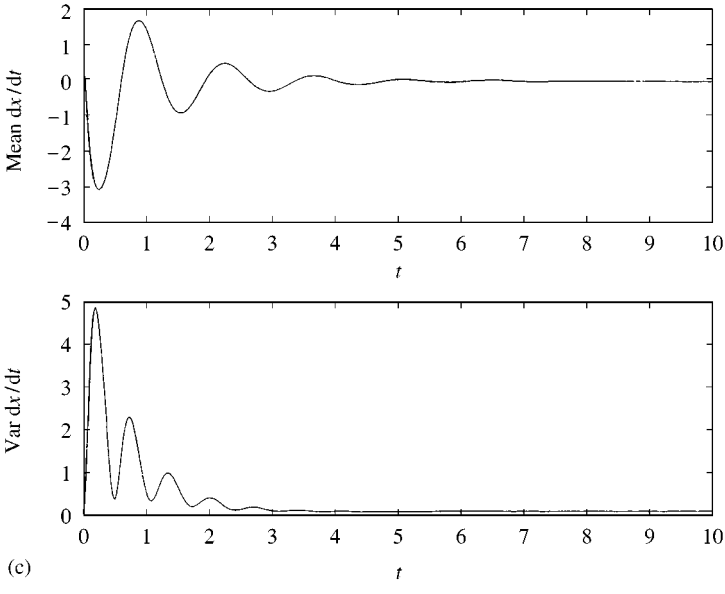

Figure 13. Continued.

non-linear systems, the current procedure is accurate enough for predicting multi-periodic, almost periodic and chaotic orbits of the evolving flow. In case of purely stochastic excitations in the form of Gaussian white-noise processes non-linearity in the vector field leads to non-Gaussianity of the TPD. The present scheme has the potential to correctly describe non-Gaussianity and non-stationarity of the response TPDs.

The technique may further be exploited for consistent derivations of higher order linearization schemes in deterministic and stochastic cases. This is achieved by including more and more terms in the short-time averaged Taylore or Ito–Taylor (as the case may be) expansions, which is necessary for linearizing the non-linear terms in the vector field. Limited results showing comparisons of TPDs obtained via the present set of schemes with the available exact analytical expressions in the stationary regime are also a pointer to the accuracy and correctness of this new linearization procedure. In case of combined stochastic and deterministic excitations, all the three features of non-stationarity, non-Gaussianity and multimodality of the response TPD are clearly brought out. Among the two different numerical methods proposed in sections 4.1 and 4.2, method 1 (section 4.1) combining the linearization scheme with the half-drift implicit scheme is observed to be more accurate than method 2, i.e., the simulation procedure of section 4.2. Method 2 is, however, found to be much more efficient computationally. The reason behind this is the way in which the conditionally Gaussian non-stationary TPDs are computed from the associated Fokker–Planck equation. Given a particular vector field with the associated parameters completely defined, the functional form of these conditional TPDs does not change from point to point or from time to time. However, one has to use very accurate random number

generators with double-precision arithmetic to ensure accuracy. Here it may be relevant to point out that an expansion of the Fokker–Planck operator over a very short time interval, sometimes referred to as the path integral formalism [11, 12], also leads to conditionally Gaussian TPDs as in method 2 of the present study. However, a disadvantage of the path integral method is that, over a short time interval, the conditionally Gaussian TPD does not take into account the cross-correlation of x_{i+1} and $\dot{x}_{i+1}$. Such a shortcoming is, however, overcome in the present scheme (method 2), where this cross-correlation is duly reflected.

A major advantage of the new linearization procedure is its semi-analytical nature, which may be suitably exploited to obtain more information about the original flow. In particular, it may be noted that the tangent spaces of the non-linear vector field at different solution points. A topological analysis of these tangent spaces is therefore necessary to lay appropriate mathematical foundations for the principles of conditional linearization. An important issue not yet addressed is the accumulation of local and global errors in the PSL-based implicit schemes for deterministic and stochastic cases. Other related issues, still unaccomplished, are the verifications of numerical efficiency of the proposed schemes vis-a-vis other numerical schemes and, even more importantly, stability of these algorithms especially near the boundaries of basins of attraction. Moreover, discontinuous vector fields have not been included in the present paper. In particular, extensions of the principles PSL to include Dirac delta-type discontinuity will be an interesting and useful exercise.

ACKNOWLEDGMENTS

The present study is a part of the author's post-doctoral work at the Institute of Engineering Mechanics, University of Innsbruck, Austria under grant no. FWF 11498-MAT. The author wishes to thank Prof. G. I. Schueller for his encouragement.

REFERENCES

1. R. N. Iyengar and D. Roy 1998 *Journal of Sound and Vibration* **211**, 843–875. New approaches for the study of nonlinear oscillators.
2. R. N. Iyengar and D. Roy 1998 *Journal of Sound and Vibration* **211**, 877–906. Extensions of the phase space linearization method.
3. R. N. Iyengar and D. Roy 1999 *Proceedings of IUTAM Symposium on Nonlinearity and Stochastic Structural Dynamics*. Dordrecht: Kluwer Academic Press. Application of conditional linearization in the study of nonlinear systems.
4. E. Simiu and M. R. Frey 1996 *Journal of Engineering Mechanics* **122**, 263–270. Melinikov processes and noise-induced exits from well.
5. T. Kapitaniak 1990 *Chaos in Systems with Noise*. Singapore: World Scientific.
6. T. Kapitaniak 1991 *International Journal of Bifurcation and Chaos* **1**, 357–363. The loss of chaos in a quasiperiodically forced nonlinear oscillator.
7. Y. K. Lin and G. Q. Cai 1995 *Probabilistic Structural Dynamics*: *Advanced Theory and Applications*. New York: McGraw-Hill.
8. P. E. Kloeden and E. Platen 1992 *Numerical Solutions of Stochastic Differential Equations*. Berlin: Springer-Verlag.

9. P. E. KLOEDEN, E. PLATEN and H. SCHURZ 1994 *Numerical Solution of Stochastic Differential Equations Through Computer Experiments*. Berlin: Springer-Verlag.
10. A. ASKAR, S. R. KOYLUOGLU, K. NIELSEN and A. S. CAKMAK 1996 *Probabilistic Engineering Mechanics* **11**, 63–72. Faster simulation methods for nonstationary random vibrations of nonlinear m.d.o.f. systems.
11. A. NAESS and J. M. JOHNSON 1991 Proceedings of IUTAM Symposium on Nonlinear Stochastic Mechanics, pp. 401–414. Response statistics of nonlinear dynamic systems by path integration.
12. H. RISKEN 1989 *The Fokker Planck Equation: Methods of Solution and Applications*. Berlin: Springer.
13. D. R. J. CHILLINGWORTH 1976 *Differential Topology with a View to Applications*. London: Pitman.
14. J. HALE 1980 *Ordinary Differential Equations*. New York: Springer-Verlag.
15. C. GOFFMAN and G. PEDRICK 1965 *First Course in Functional Analysis*. Englewood Cliffs, NJ: Prentice-Hall.
16. N. C. NIGAM 1983 *Introduction to Random Vibrations*. Cambridge: MIT Press.
17. R. N. IYENGAR 1991 *Physics Letters A* **154**, 357–360. Stochastic characterization of Chaos in nonlinear system.
18. J. B. ROBERTS and P. D. SPANOS 1990 *Random Vibration and Statistical Linearization*. Chichester: John Wiley & Sons.

APPENDIX A: AN EXPLANATION OF THE SYMBOLS USED IN STOCHASTIC TAYLOR EXPANSION

Consider vector Ito stochastic process $\bar{X}_t = \{X_t^i | i = 1, 2, \ldots, d\} \in R^d$ driven by a vector Wiener process $\bar{W}_t = \{W_t^j | j = 1, 2, \ldots, m\}$, where d and m are positive integers. The Ito stochastic differential equations are

$$X_t^i = X_{t_0}^i + \int_{t_0}^t a^i(s, \bar{X}_s)\,\mathrm{d}s + \sum_{j=1}^m \int_{t_0}^t b^{ij}(s, \bar{X}_s)\,\mathrm{d}W_s^j. \tag{A1}$$

An Ito–Taylor expansion of X_t^i may be performed by repeatedly applying the Ito formula (see below) to the drift coefficients $a^i(s, \bar{X}_s)$ and diffusion coefficients $b^{ij}(s, \bar{X}_s)$. The Ito formula for a sufficiently differentiable scalar function $f(\bar{X}_t, t)$ is

$$f(\bar{X}_t, t) = f(\bar{X}_{t_0}, t) + \int_{t_0}^t L^0 f(\bar{X}_s, s)\,\mathrm{d}s + \sum_{j=1}^m \int_{t_0}^t L^{1j} f(\bar{X}_s, s)\,\mathrm{d}W_s^j, \tag{A2}$$

where the operators L^0 and L^{1j} are defined as

$$L^0 = \frac{\partial}{\partial t} + \sum_{i=1}^d a^i \frac{\partial}{\partial X^i} + 0{\cdot}5 \sum_{i,k=1}^d \sum_{j=1}^m b^{ij} b^{kj} \frac{\partial^2}{\partial X^i \partial X^k},$$

$$L^{1j} = \sum_{i=1}^d b^{ij} \frac{\partial}{\partial X^i}. \tag{A3}$$

Multiple stochastic integrals: While deriving the stochastic Taylor expansion, one comes across multiple stochastic integrals of the type $\int_{t_0}^{t}\int_{t_0}^{s_l}\int_{t_0}^{s_{l-1}}\cdots\int_{t_0}^{s_2} \mathrm{d}W_{s_l}^{j_1}\cdots \mathrm{d}W_{s_{l-1}}^{j_{l-1}}\,\mathrm{d}W_{s_l}^{j_l}$ where the set of superscripts $\alpha = [j_1\, j_2, \ldots, j_l\} \in M$ is called a multi-index, M is the set of multi-indices, $j_i \in \{0, 1, \ldots, m\}$, $i \in \{1, 2, \ldots, l\}$. Here it is important to note that $W_t^0 = t$, by definition. The positive integer $l = l(\alpha) \in \{1, 2, \ldots\}$ is called the length of the multi-index α. For completeness of definition, $v \in M$ denotes a multi-index of length zero. In addition, $n(\alpha)$ is defined to be the number of components in α which are equal to zero. For any $\alpha \in M$ with $l(\alpha) \geqslant 1$, one defines $\alpha -$ and $-\alpha$ to be the multi-indices in M by deleting the last and first components of α respectively.

Now the multiple Ito integral I_α on a right continuous stochastic process $f(t, \omega)$, $t \geqslant 0$ with left-hand limits is recursively defined as follows. If $\rho(\omega)$ and $\tau(\omega)$ are two stopping times with $0 \leqslant \rho \leqslant \tau$ w.p.l, then

$$\begin{aligned} I_\alpha[f(.)]_{\rho,\tau} &= f(\tau), \quad l(\alpha) = 0, \\ &= \int_\rho^\tau I_{\alpha-}[f(.)_{\rho,s}\,\mathrm{d}s, \quad l(\alpha) \geqslant 1, j_l = 0, \\ &= \int_\rho^\tau I_{\alpha-}[f(.)_{\rho,s}\,\mathrm{d}W_s^{ji}, \quad l(\alpha) \geqslant 1, j_l \geqslant 0. \end{aligned} \tag{A4}$$

If $f(t) = 1$, then $I_\alpha[f(.)]_{\rho,s}$ is often abbreviated as $I_{\alpha,\rho,s}$. Moreover, the two stopping times are also removed sometimes from the subscripts in case they are clear from the context. It may be useful to consider the following illustrations:

$$I_{(0)}[f(.)]_{t_i,t_{i+1}} = \int_{t_i}^{t_{i+1}} f(s)\,\mathrm{d}s, \qquad I_{(1)}[f(.)]_{t_i,t_{i+1}} = \int_{t_i}^{t_{i+1}} f(s)\,\mathrm{d}W_s^1,$$

$$I_{(0,2,1),0,t} = \int_0^t \int_0^{s_3} \int_0^{s_2} \mathrm{d}s_1\,\mathrm{d}W_{s_2}^2\,\mathrm{d}W_{s_3}^1. \tag{A5}$$

Coefficient functions: Like the multiple Ito integrals, the Ito coefficient function, f_α, are also defined recursively as

$$\begin{aligned} f_\alpha &= f, \qquad l(\alpha) = 0, \\ &= L^{1j_1} f_{-\alpha}, \qquad l(\alpha) \geqslant 1 \end{aligned} \tag{A6}$$

for each $\alpha = \{j_1, j_2, \ldots, j_l\}$ and the function f is at least C^h, $h = l(\alpha) + n(\alpha)$. The operator L^{1j_1} is as defined in equation (A3) with the superscript j replaced by j_1. As an illustration, consider an one-dimensional case, $d = m = 1$ for $f(t, x) \equiv x$. Then

from equation (A6), one can write down the following Ito coefficient functions:

$$f_{(0)} = a, \qquad f_{[1]} = b, \qquad f_{(1,1)} = bb', \qquad f_{(0,1)} = ab' + 0{\cdot}5b^2b'', \tag{A7}$$

where the prime $'$ denotes the derivative w.r.t. the variable x.

Hierarchical and remainder sets: A subset $A \subset M$ is a hierarchical set if A is non-empty, the multi-indices in A are uniformly bounded in length (i.e., $l(\alpha) < \infty$ if $\alpha \in A$) and if $-\alpha \in A$ for each $\alpha \in A \backslash \{v\}$. Note that $\{v\}$ is the null index set. If an Ito–Taylor expansion is performed for a given hierarchical set, then the remainder set consists of all the remaining higher order multiple stochastic integrals. More precisely, for any given hierarchical set A, the remainder set $\mathfrak{R}(A)$ is defined as

$$\mathfrak{R}(A) = \{\alpha \in M \backslash A | \ -\alpha \in A\}. \tag{A8}$$

For example, the sets $\{v\}$, $\{v, (0), (1)\}$, $\{v, (0), (1), (1, 1)\}$ are hierarchical sets. Also for $m = 1$, one has, among others, the following remainder sets:

$$\mathfrak{R}(\{v\}) = \{(0), (1)\}, \qquad \mathfrak{R}(\{v, (0), (1)\}) = \{(0, 0), (0, 1), (1, 0), (1, 1)\},$$

$$\mathfrak{R}(\{v, (0), (1), (1, 1)\}) = \{(0, 0), (0, 1), (1, 0), (0, 1, 1), (1, 1, 1)\}. \tag{A9}$$

Similar such symbols are available for Stratonovich–Taylor expansion as well.